LA-UR-21-25435
Approved for public release; distribution is unlimited.

Title: An Astronomer's Journey into Radiography

Author(s): Hovey, Luke Douglas

Intended for: Job Talk for MSTS

Issued: 2021-06-10

Disclaimer:
Los Alamos National Laboratory, an affirmative action/equal opportunity employer, is operated by Triad National Security, LLC for the National Nuclear Security Administration of U.S. Department of Energy under contract 89233218CNA000001. By approving this article, the publisher recognizes that the U.S. Government retains nonexclusive, royalty-free license to publish or reproduce the published form of this contribution, or to allow others to do so, for U.S. Government purposes. Los Alamos National Laboratory requests that the publisher identify this article as work performed under the auspices of the U.S. Department of Energy. Los Alamos National Laboratory strongly supports academic freedom and a researcher's right to publish; as an institution, however, the Laboratory does not endorse the viewpoint of a publication or guarantee its technical correctness.

Luke Hovey: 10 June, 2021

An Astronomer's Journey into Radiography

Image Credit: Hubble Heritage

Overview/Motivation

- A proper motion measurement of the young supernova remnant 0509-67.5 in the Large Magellanic Cloud
  - Image Processing
  - Linking Measured Observational Results to calculations and hydrodynamic Simulations
- Measuring the Spot Blur on Axis-2 at the Dual-Axis Radiographic Hydrodynamic Test Facility (DARHT)
  - Use of the Bayesian Inference Engine (BIE)
  - Real-world analysis of DARHT data

Overview/Motivation

- A proper motion measurement of the young supernova remnant 0509-67.5 in the Large Magellanic Cloud
  - Image Processing
  - Linking Measured Observational Results to calculations and hydrodynamic Simulations
- Measuring the Spot Blur on Axis-2 at the Dual-Axis Radiographic Hydrodynamic Test Facility (DARHT)
  - Use of the Bayesian Inference Engine (BIE)
  - Real-world analysis of DARHT data

Measuring Shock Speeds in a Young Supernova Remnant
Image Reductions/Processing

Advanced Camera for Surveys(ACS)

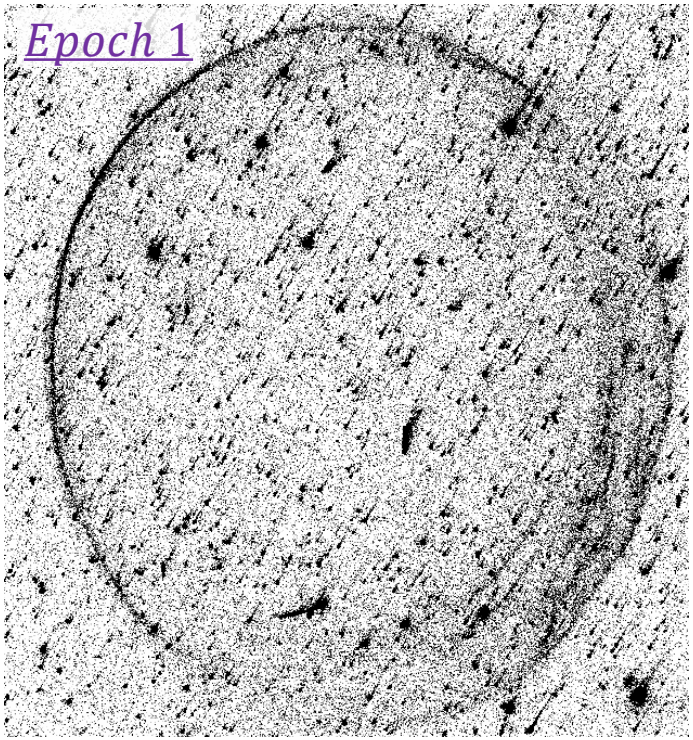

$S_{ACS} = 0.05''$/Pixel

Wide Field Planetary Camera 2(WFPC2)

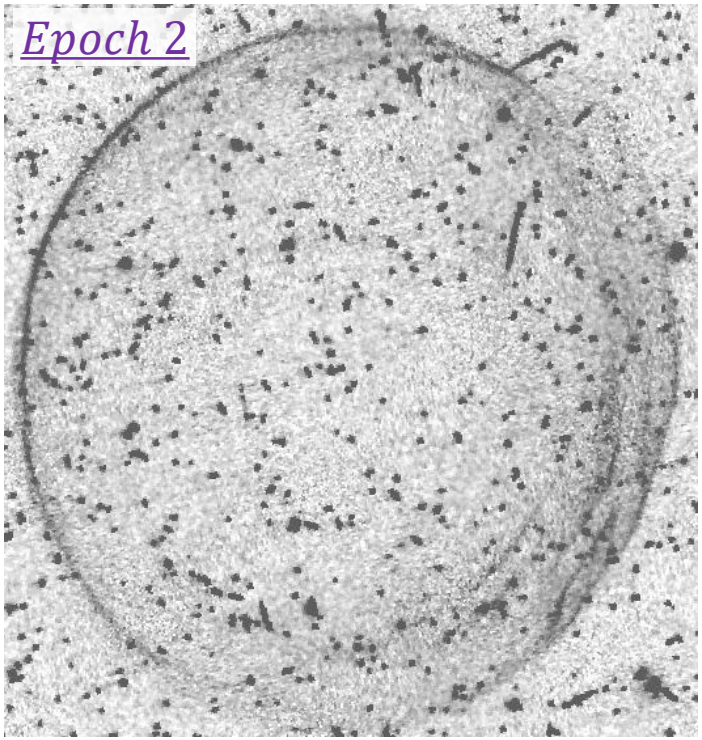

$S_{WFPC2} = 0.10''$/Pixel

Measuring Shock Speeds in a Young Supernova Remnant
Image Reductions/Processing

Advanced Camera for Surveys(ACS)

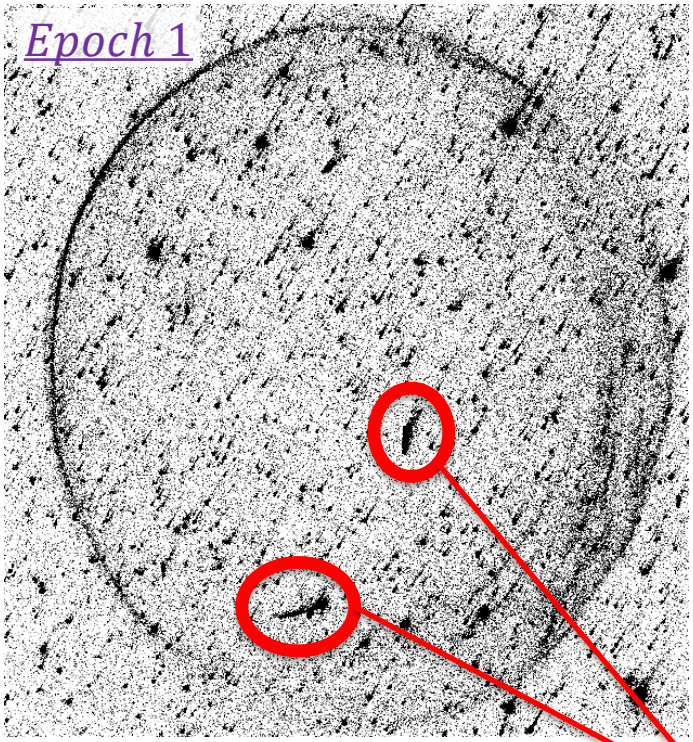

$S_{ACS} = 0.05''$/Pixel

Wide Field Planetary Camera 2(WFPC2)

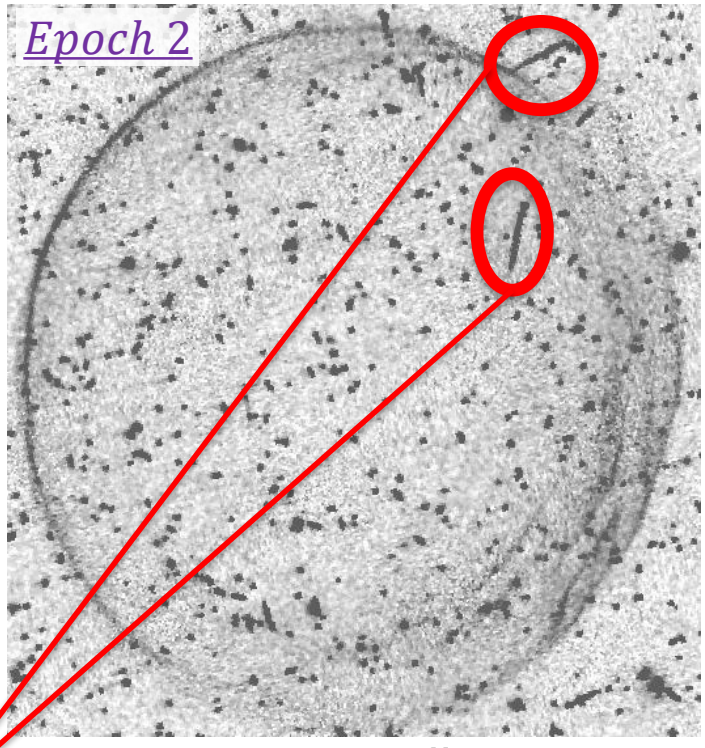

$S_{WFPC2} = 0.10''$/Pixel

Remove Cosmic Rays

Measuring Shock Speeds in a Young Supernova Remnant
Image Reductions/Processing

Advanced Camera for Surveys(ACS)

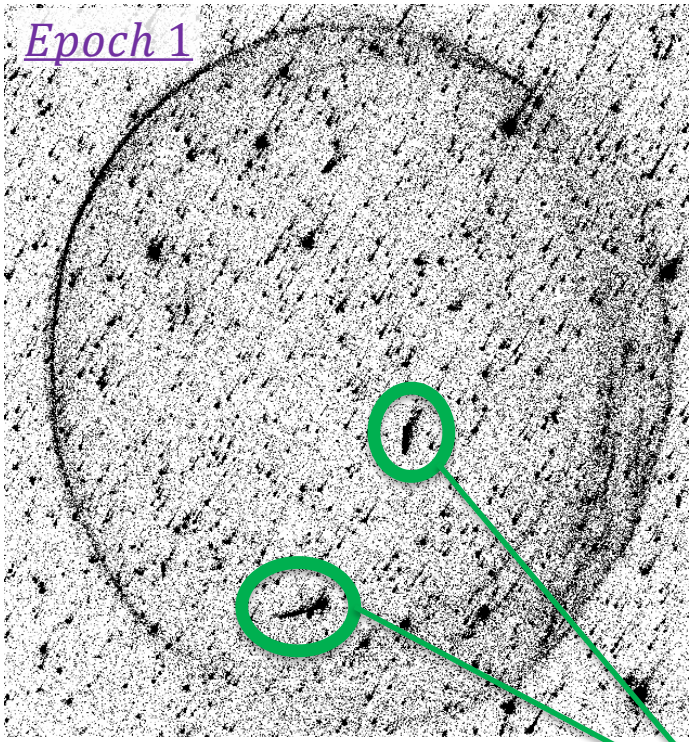

$S_{ACS} = 0.05''$/Pixel

Wide Field Planetary Camera 2(WFPC2)

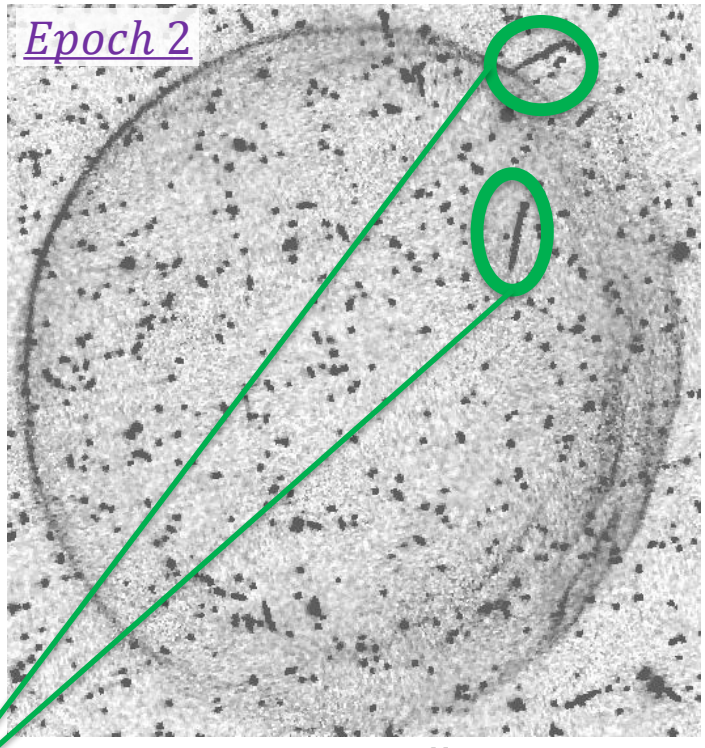

$S_{WFPC2} = 0.10''$/Pixel

Remove Cosmic Rays

Correct For Geometric Distortion

Measuring Shock Speeds in a Young Supernova Remnant
Image Reductions/Processing

Advanced Camera for Surveys(ACS)

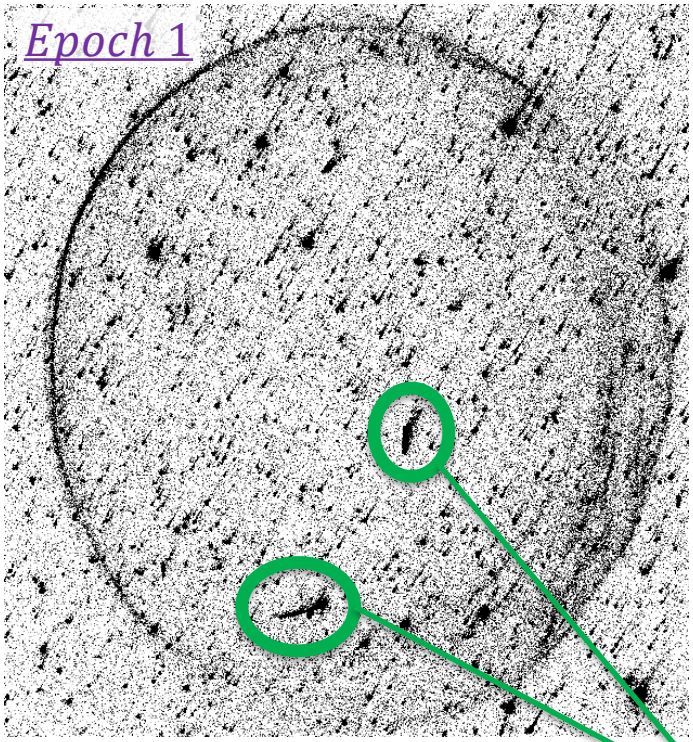

$S_{ACS} = 0.05''$/Pixel

Wide Field Planetary Camera 2(WFPC2)

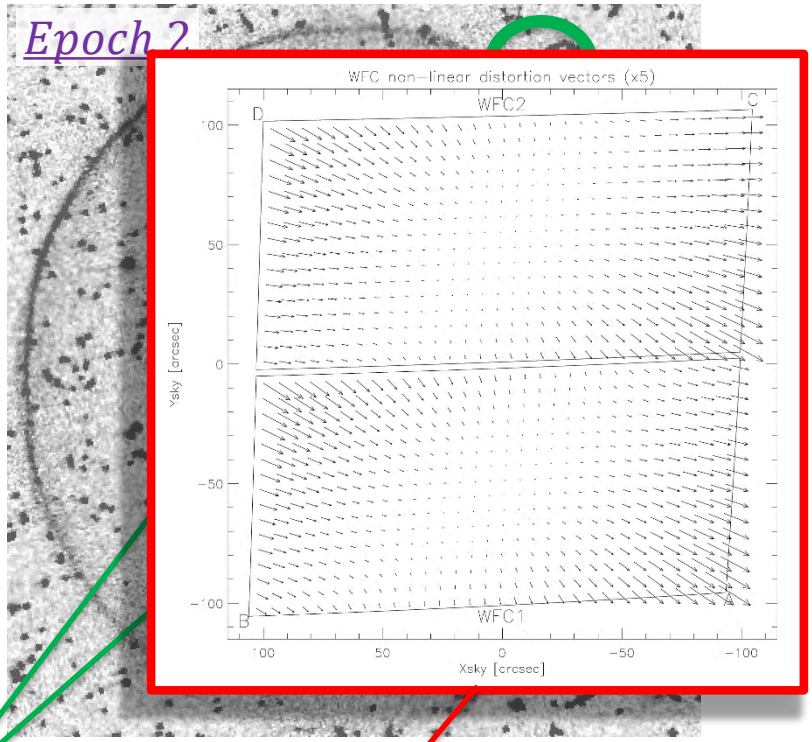

$S_{WFPC2} = 0.10''$/Pixel

Remove Cosmic Rays

Correct For Geometric Distortion

Measuring Shock Speeds in a Young Supernova Remnant
Image Reductions/Processing

Advanced Camera for Surveys(ACS)

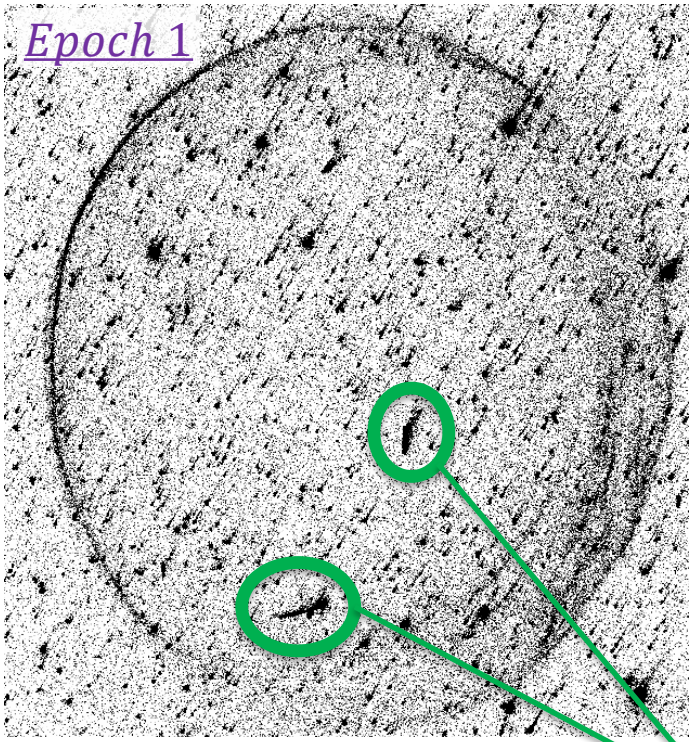

$S_{ACS} = 0.05''$/Pixel

Wide Field Planetary Camera 2(WFPC2)

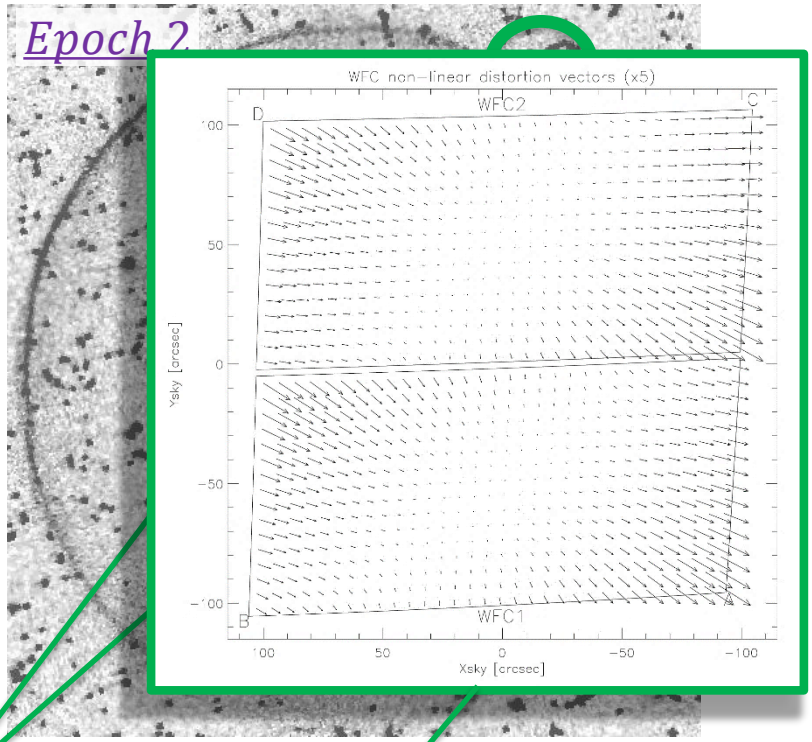

$S_{WFPC2} = 0.10''$/Pixel

Remove Cosmic Rays
Correct For Geometric Distortion
Flat-Field/Bias-Gain Correction/Destriping

Measuring Shock Speeds in a Young Supernova Remnant
Image Reductions/Processing

Advanced Camera for Surveys(ACS)

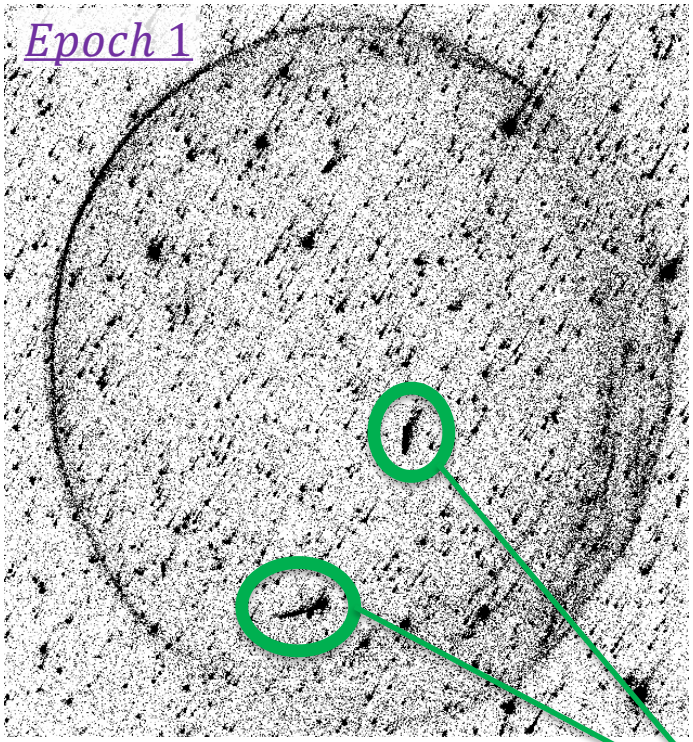

$S_{ACS} = 0.05''$/Pixel

Wide Field Planetary Camera 2(WFPC2)

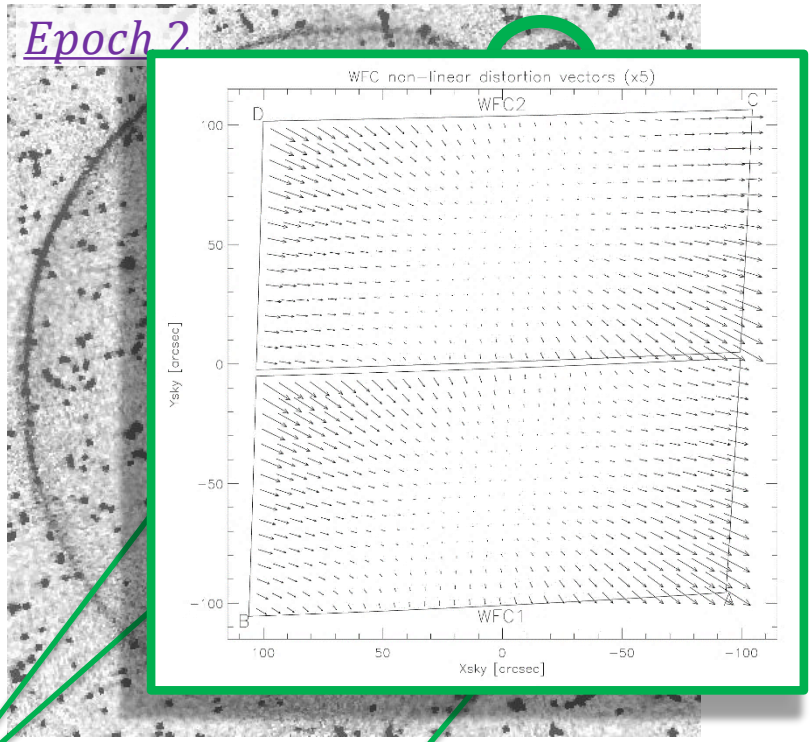

$S_{WFPC2} = 0.10''$/Pixel

Remove Cosmic Rays
Correct For Geometric Distortion
Flat-Field/Bias-Gain Correction/Destriping
Match Point Spread Functions(PSFs)

Measuring Shock Speeds in a Young Supernova Remnant
Image Reductions/Processing

Advanced Camera for Surveys(ACS)

Wide Field Planetary Camera 2(WFPC2)

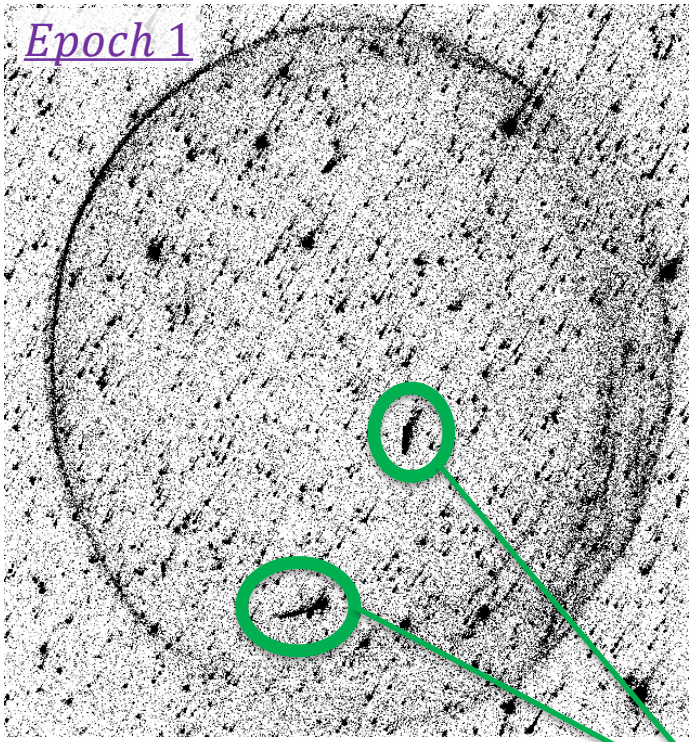

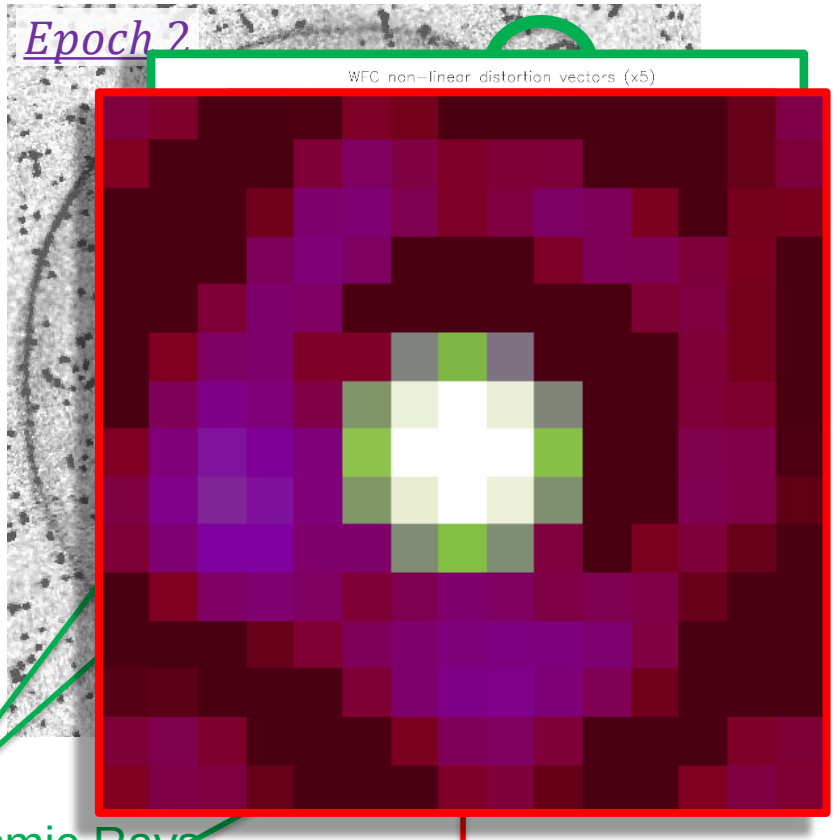

$S_{ACS} = 0.05''$/Pixel

Remove Cosmic Rays
Correct For Geometric Distortion
Flat-Field/Bias-Gain Correction/Destriping
Match Point Spread Functions(PSFs)

Measuring Shock Speeds in a Young Supernova Remnant
Image Reductions/Processing: Final Products

$Epoch$ 1-ACS

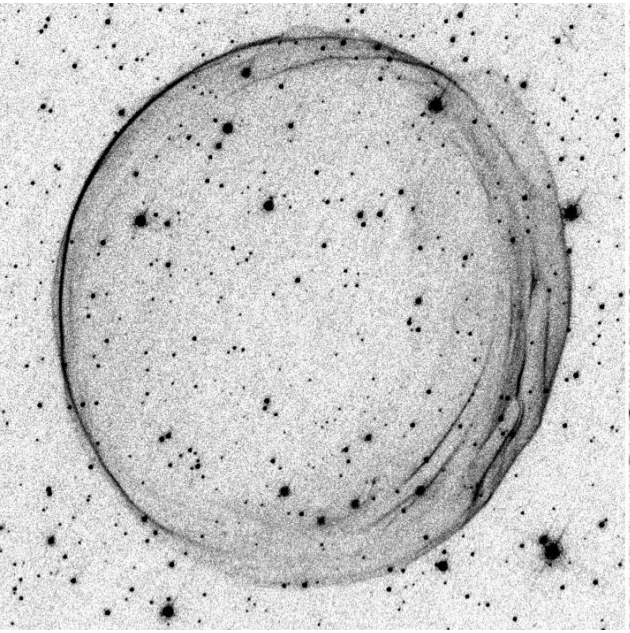

$Epoch\ 2 - WFPC2$

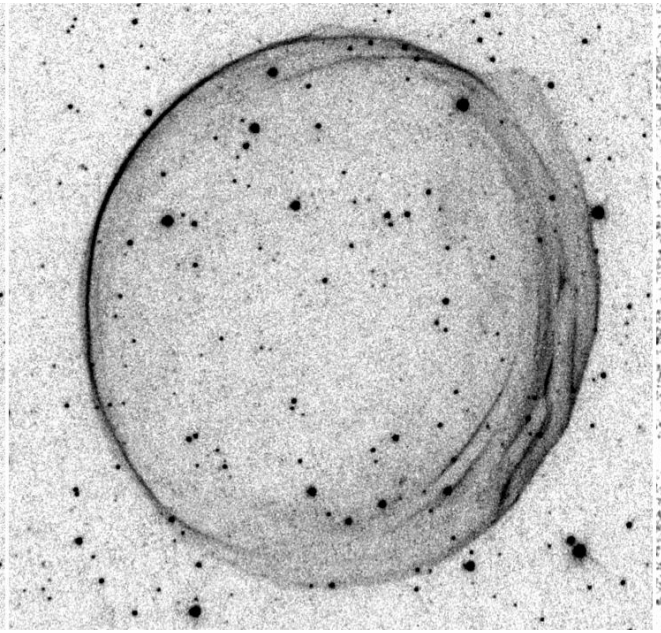

Flux-Scaled $Difference$

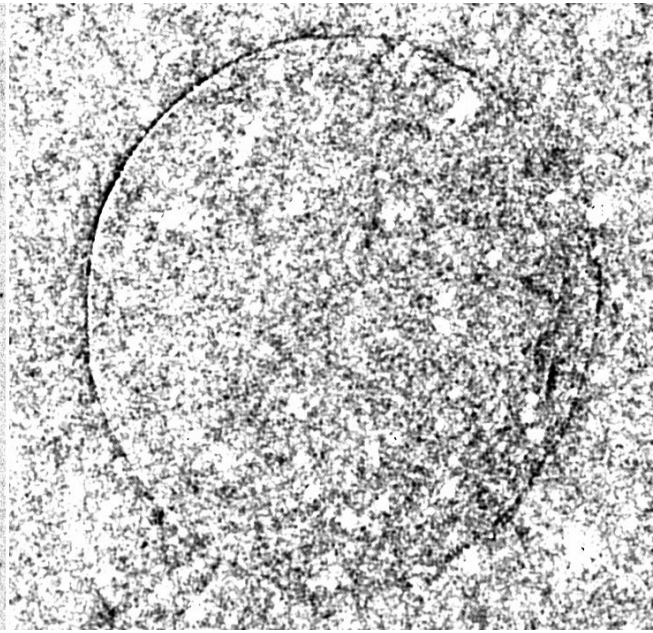

Measuring Shock Speeds in a Young Supernova Remnant

Choice of Measurement Regions

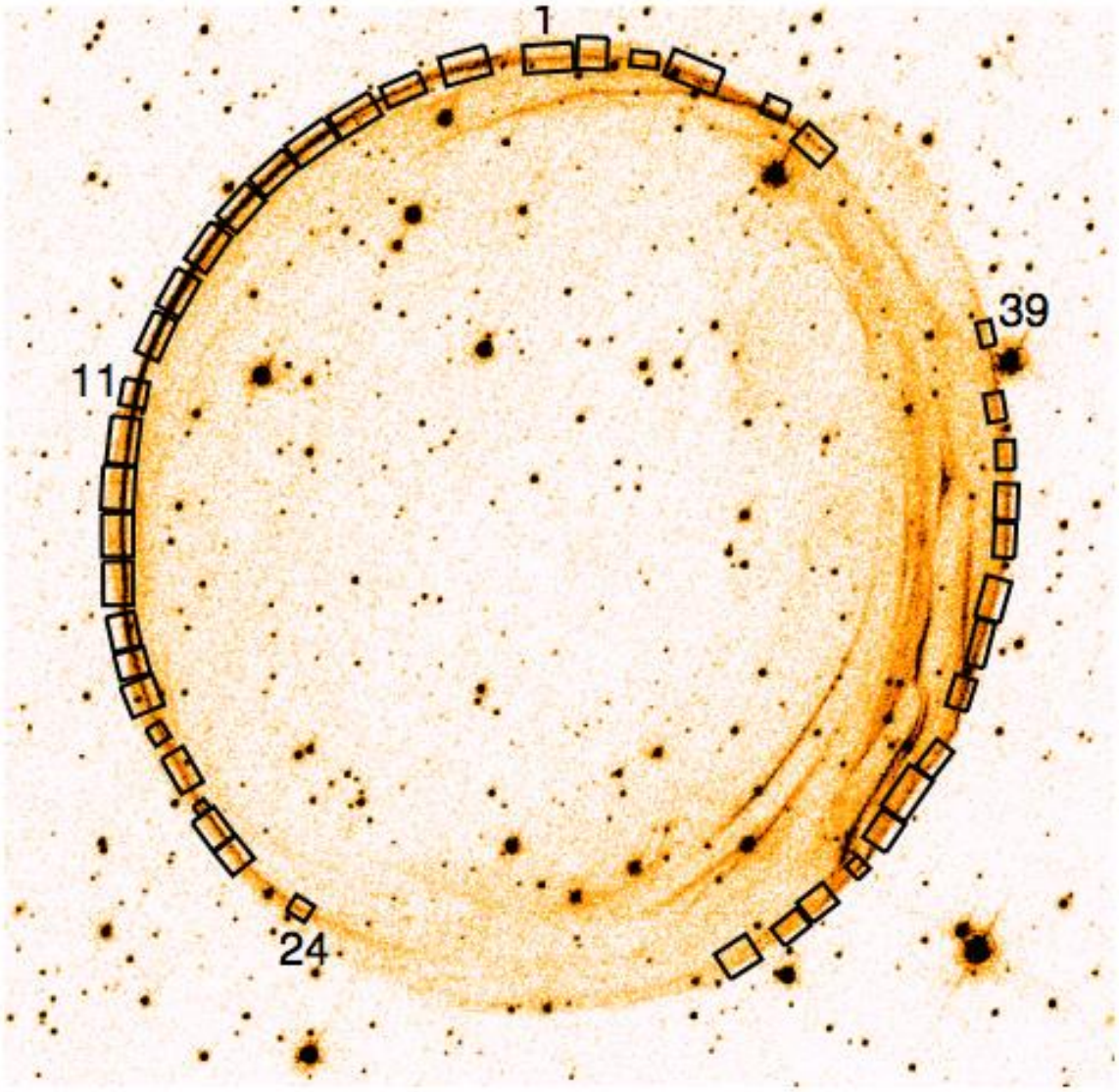

Los Alamos NATIONAL LABORATORY EST. 1943
Managed by Triad National Security, LLC for the U.S. Department of Energy's NNSA
NNSA National Nuclear Security Administration
Unclassified

Measuring Shock Speeds in a Young Supernova Remnant
Method of Measuring Proper Motion

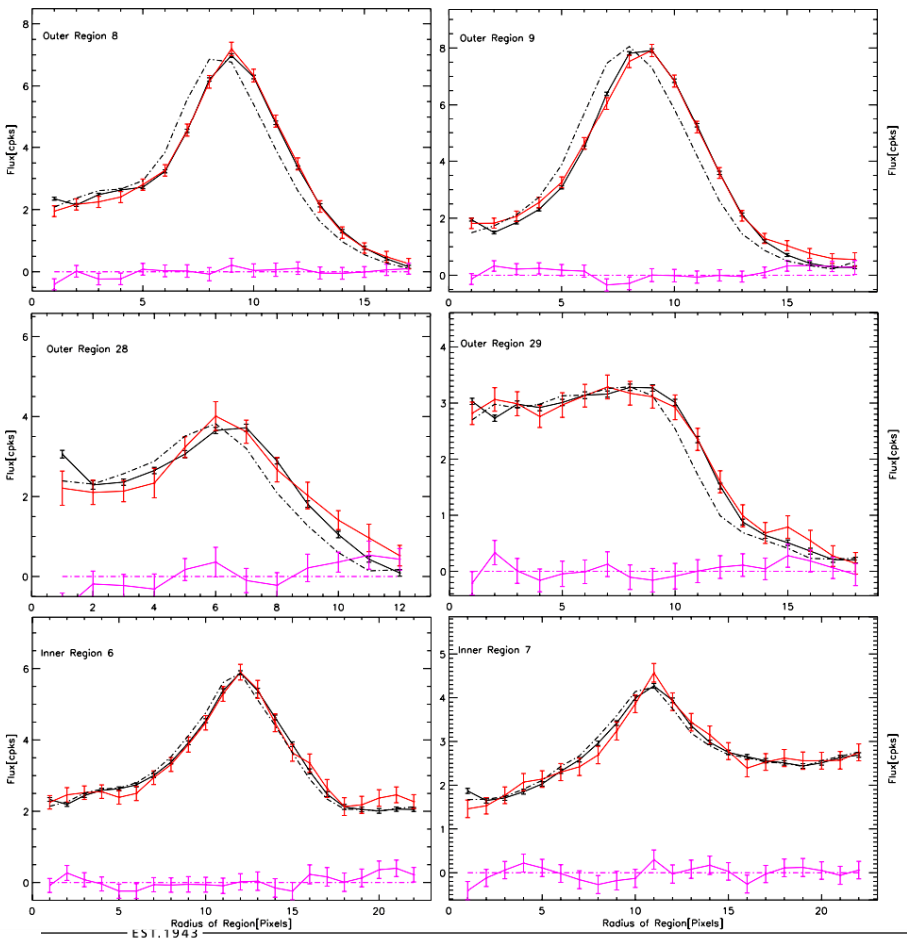

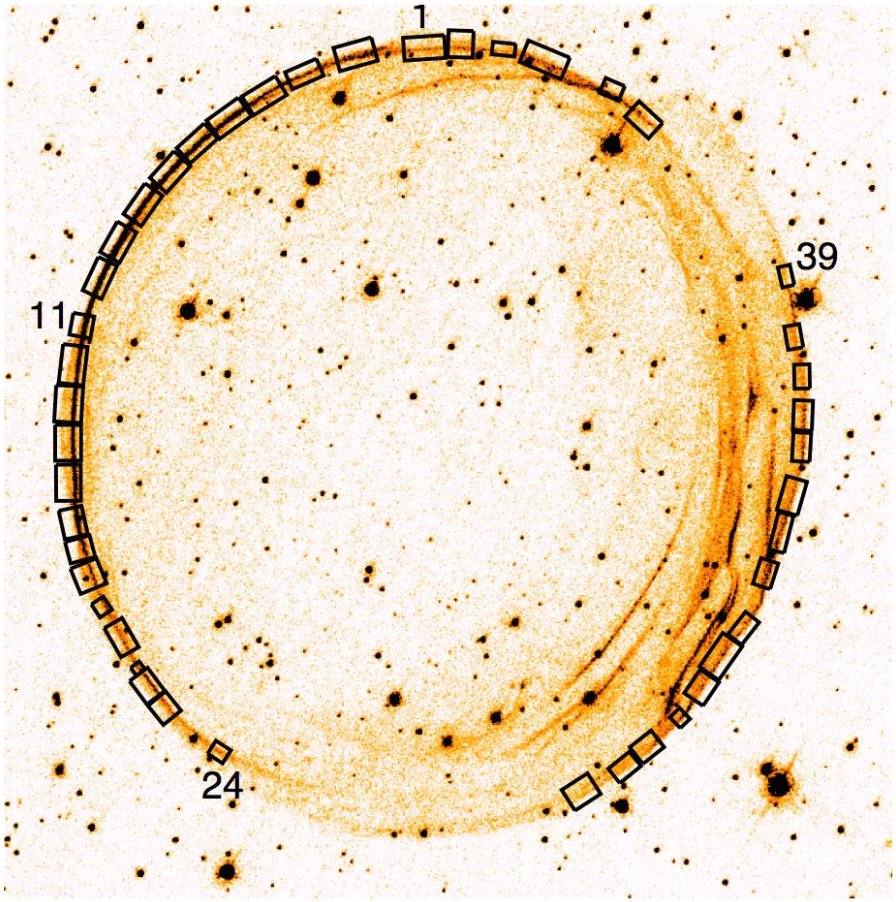

Managed by Triad National Security, LLC for the U.S. Department of Energy's NNSA

Unclassified

Measuring Shock Speeds in a Young Supernova Remnant

Results

$$d_{LMC} = 50000\ pc = 1.543 \times 10^{18} cm$$

$$\Delta t = 375\ Days = 3.24 \times 10^{7}\ Seconds$$

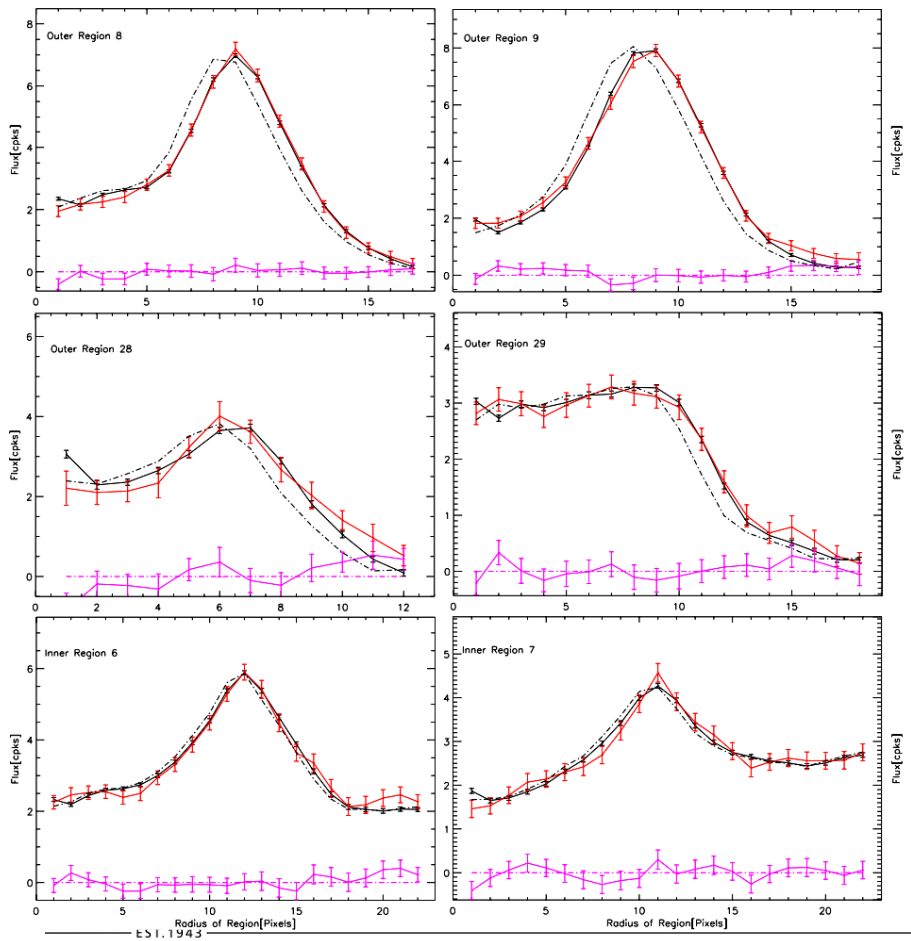

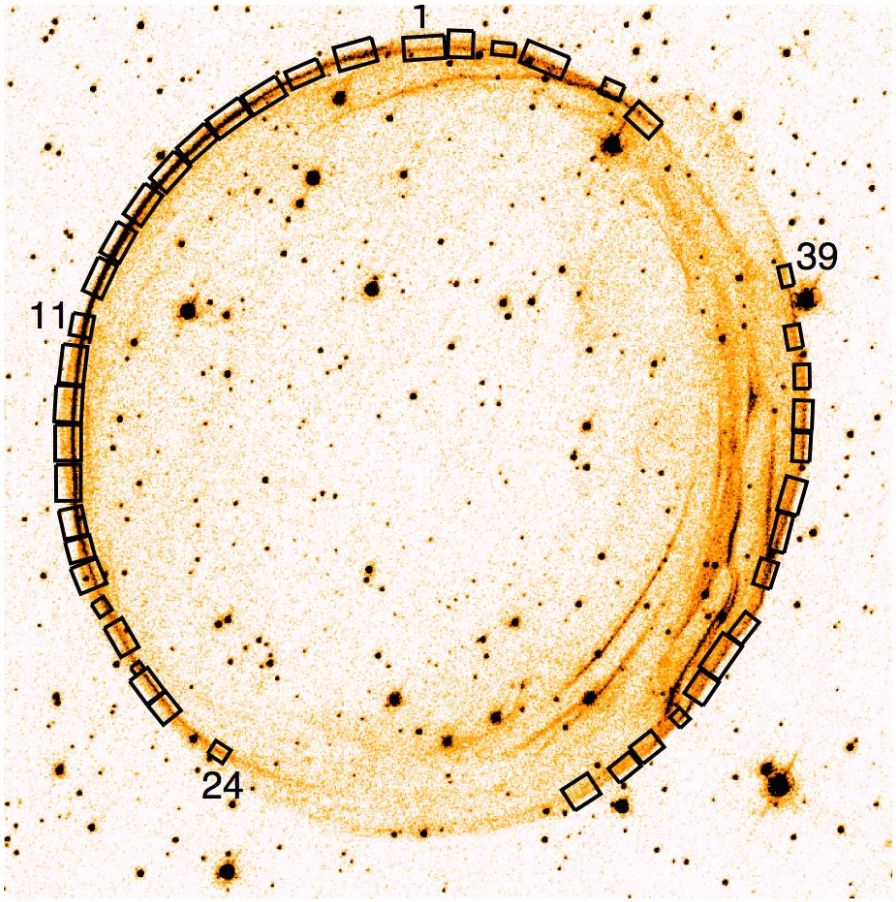

Managed by Triad National Security, LLC for the U.S. Department of Energy's NNSA

Unclassified

Measuring Shock Speeds in a Young Supernova Remnant

Results

$$d_{LMC} = 50000\ pc = 1.543 \times 10^{18} cm$$

$$\Delta t = 375\ Days = 3.24 \times 10^{7}\ Seconds$$

$$v_s = shift[pixels] \times 11544\ km\ s^{-1}$$ with $Scale = 0.05''\ per\ Pixel$

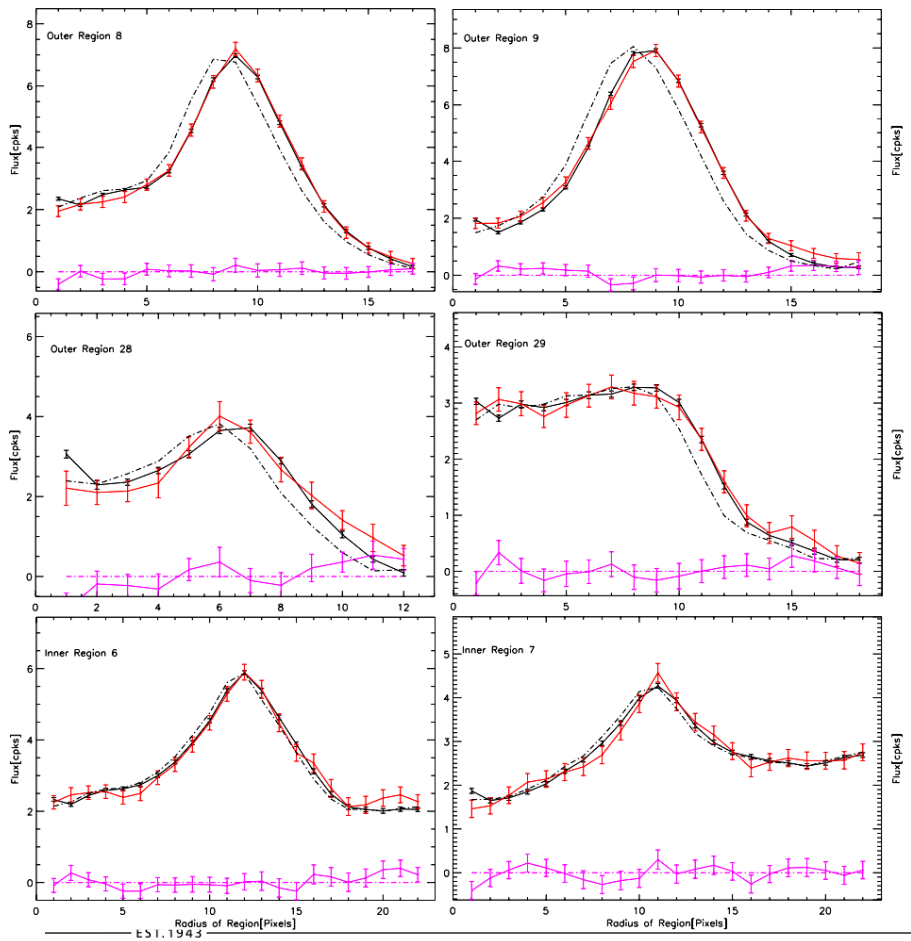

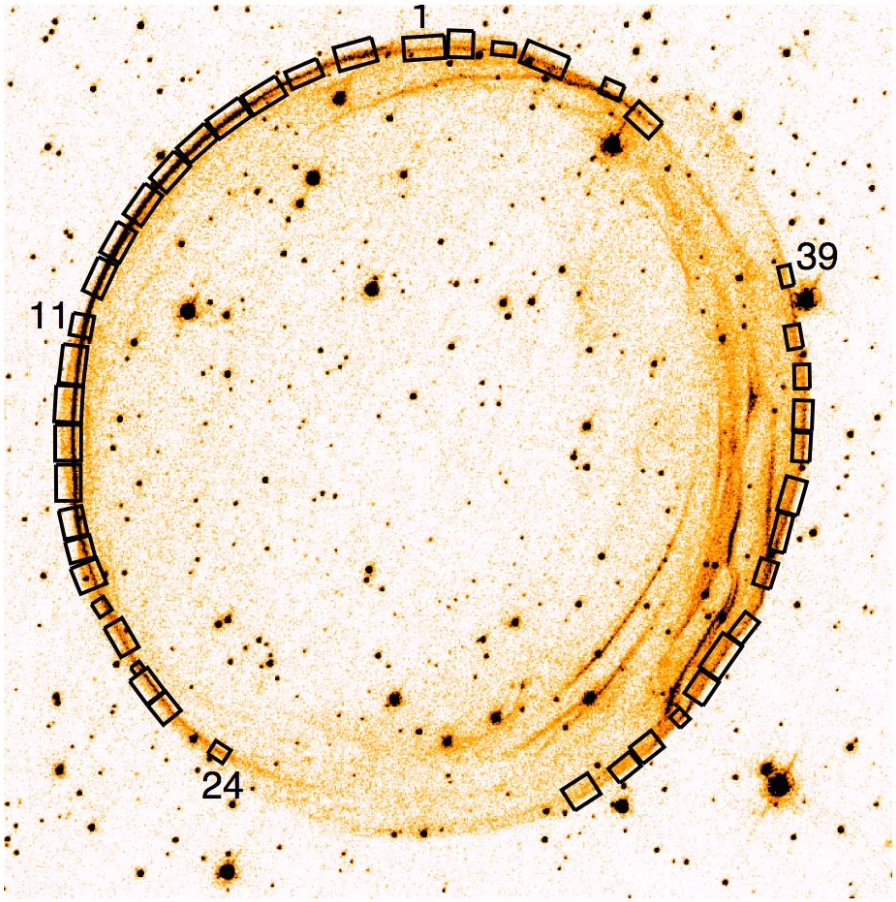

Managed by Triad National Security, LLC for the U.S. Department of Energy's NNSA

OFFICIAL USE ONLY

Measuring Shock Speeds in a Young Supernova Remnant

Results

$d_{LMC} = 50000\ pc = 1.543 \times 10^{18} cm$

$\Delta t = 375\ Days = 3.24 \times 10^{7}\ Seconds$

$v_s = shift[pixels] \times 11544\ km\ s^{-1}$ with $Scale = 0.05''\ per\ Pixel$

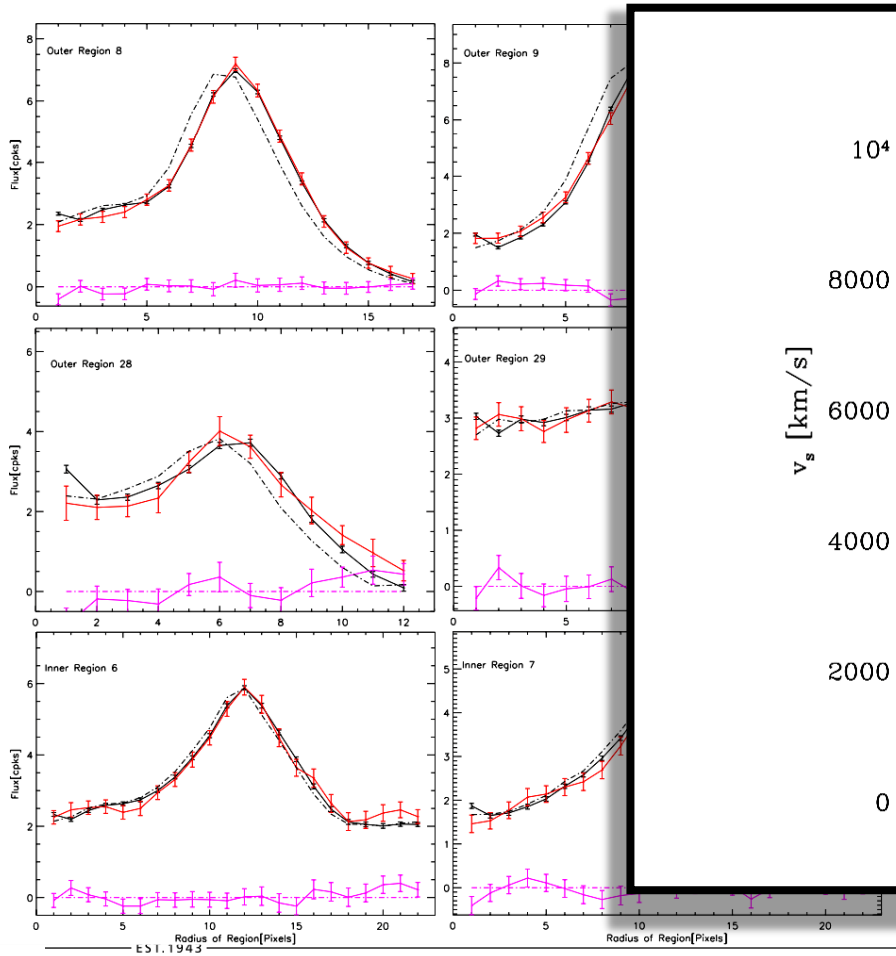

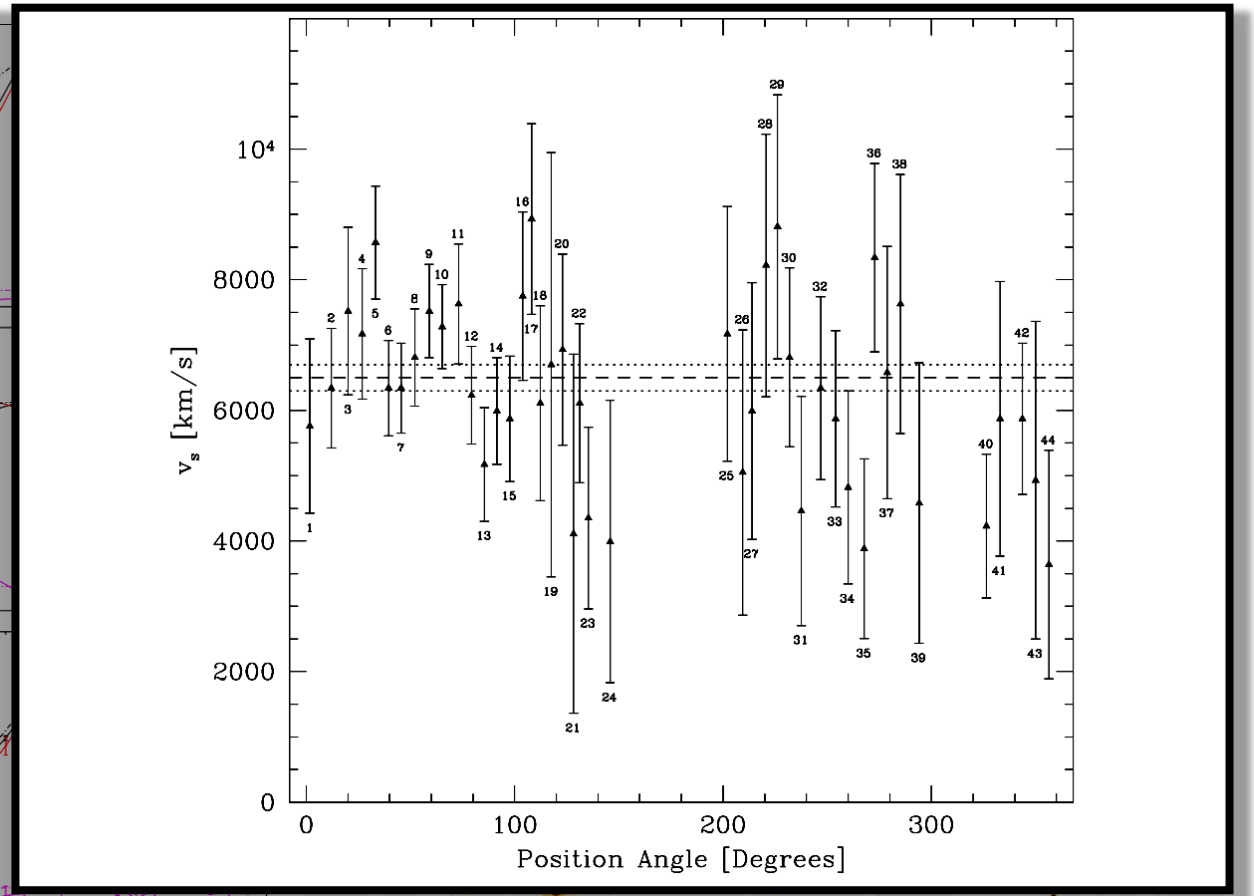

Managed by Triad National Security, LLC for the U.S. Department of Energy's NNSA

Unclassified

Measuring Shock Speeds in a Young Supernova Remnant

Results

$d_{LMC} = 50000\ pc = 1.543 \times 10^{18} cm$

$\Delta t = 375\ Days = 3.24 \times 10^{7}\ Seconds$

$v_s = shift[pixels] \times 11544\ km\ s^{-1}$ with $Scale = 0.05''\ per\ Pixel$

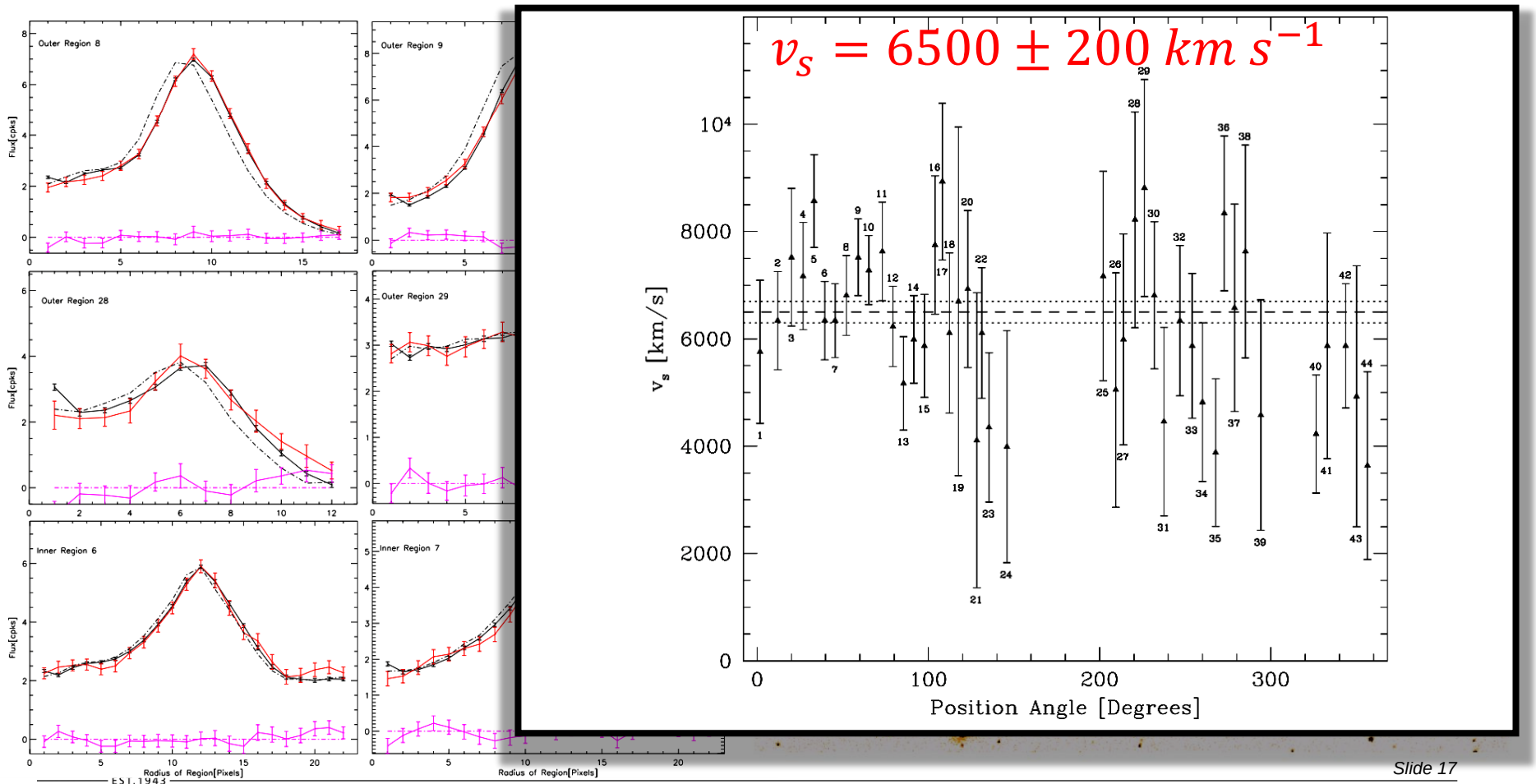

Managed by Triad National Security, LLC for the U.S. Department of Energy's NNSA

Unclassified

Measuring Shock Speeds in a Young Supernova Remnant

Calculating the Neutral Hydrogen Density

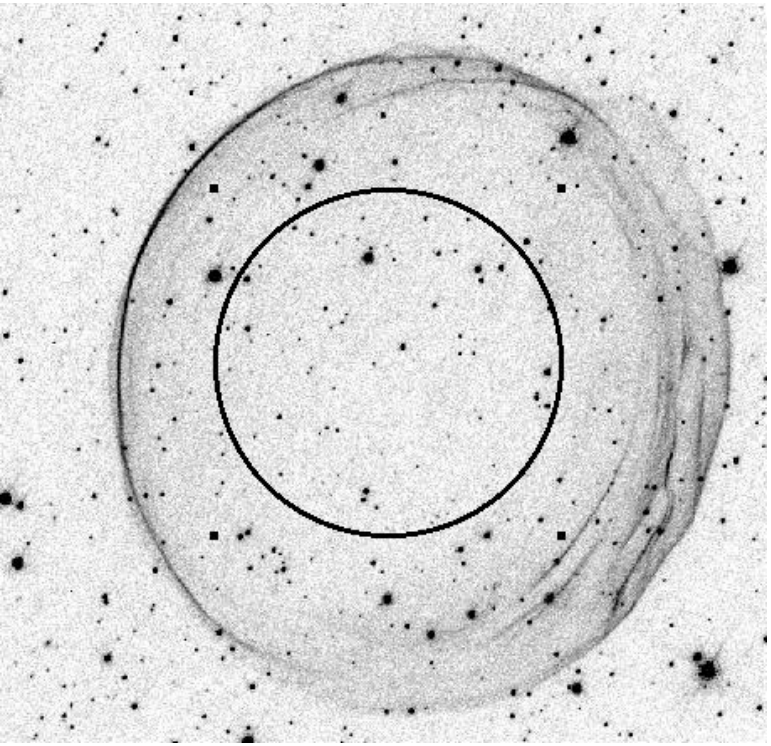

$$I_{H_\alpha} \sim \frac{1}{4\pi} n_{H_0} V_{FS} h \nu_{H_\alpha} \epsilon_{H_\alpha}$$

Measuring Shock Speeds in a Young Supernova Remnant

Calculating the Neutral Hydrogen Density

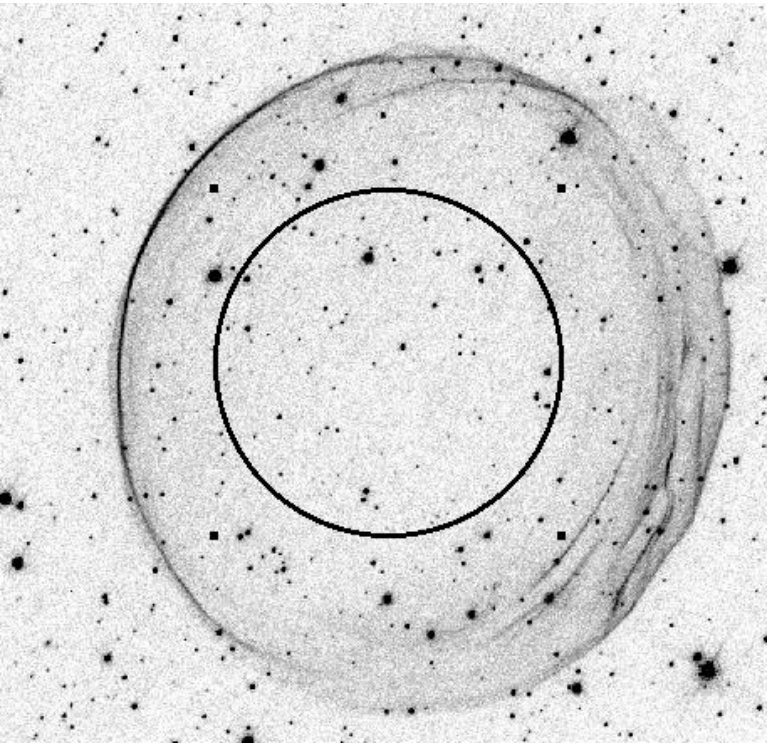

$$I_{H_\alpha} \sim \frac{1}{4\pi} n_{H_0} V_{FS} h \nu_{H_\alpha} \epsilon_{H_\alpha}$$

$$n_{H_0} = 0.084 \pm 0.003 \, (\epsilon_{H_\alpha}/0.2)^{-1} \ \mathrm{cm}^{-3}$$

$$\mu_{ISM} \sim 1.4$$

Measuring Shock Speeds in a Young Supernova Remnant

Calculating the Neutral Hydrogen Density

Results

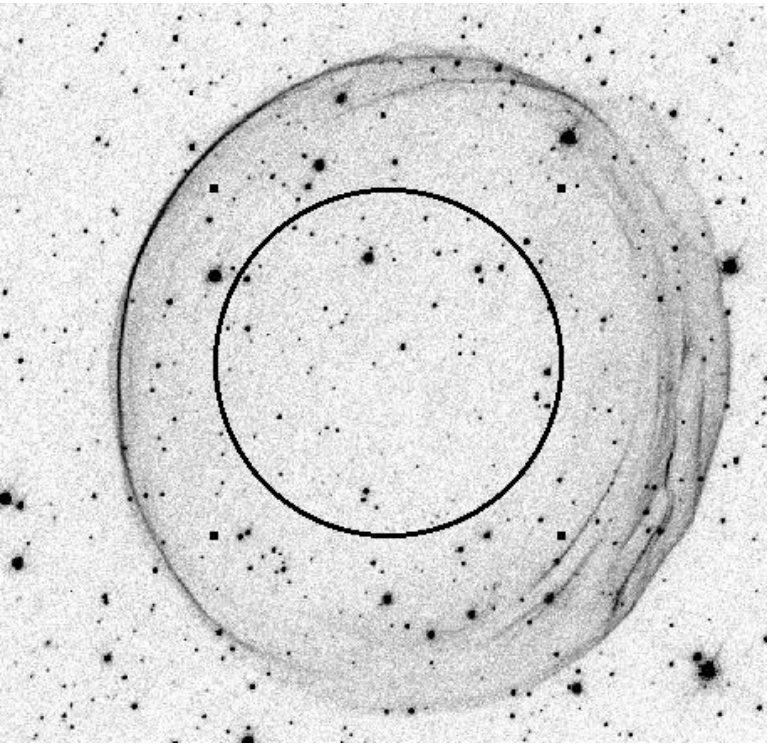

$$I_{H_\alpha} \sim \frac{1}{4\pi} n_{H_0} V_{FS} h \nu_{H_\alpha} \epsilon_{H_\alpha}$$

$$n_{H_0} = 0.084 \pm 0.003 \, (\epsilon_{H_\alpha}/0.2)^{-1} \ \mathrm{cm}^{-3}$$

$$\mu_{ISM} \sim 1.4$$

$$\rho_{H_0} \simeq 1.95 \pm 0.07 \left(\frac{\epsilon_{H_\alpha}}{0.2}\right)^{-1} \times 10^{-25} \ \mathrm{g\ cm}^{-3}$$

Hydrodynamic Model Comparison

Initial Ejecta Density Profiles

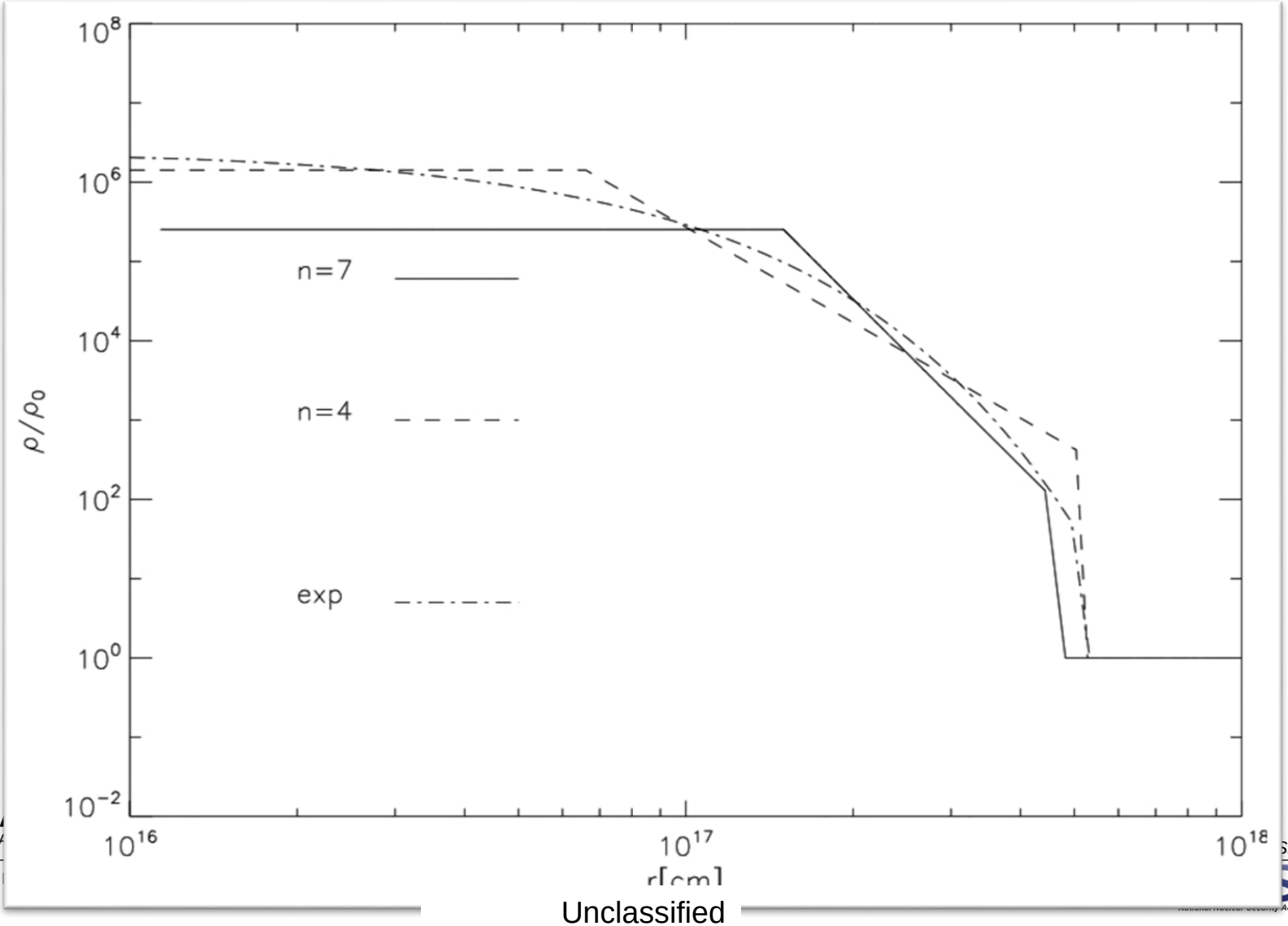

Unclassified

Hydrodynamic Model Comparison

1D Hydrodynamic Simulations

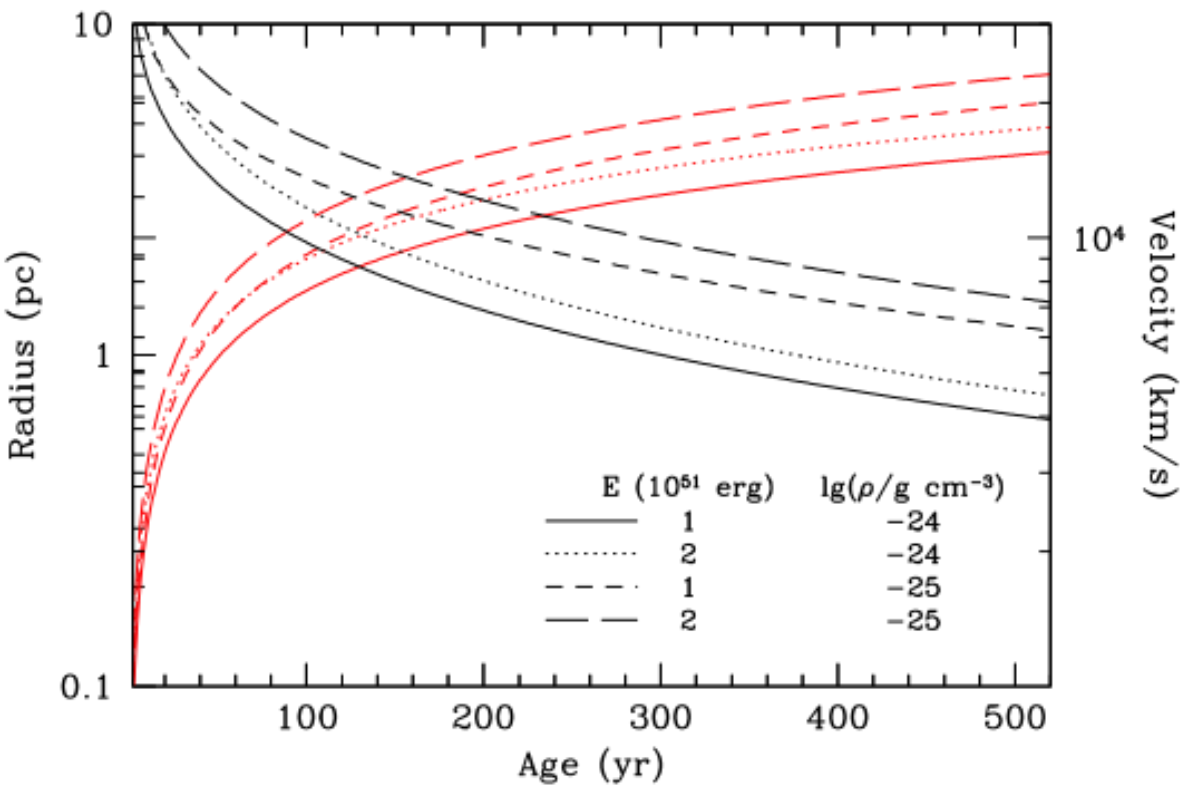

Los Alamos NATIONAL LABORATORY EST. 1943
Managed by Triad National Security, LLC for the U.S. Department of Energy's NNSA
Unclassified

Hydrodynamic Model Comparison

1D Hydrodynamic Simulations

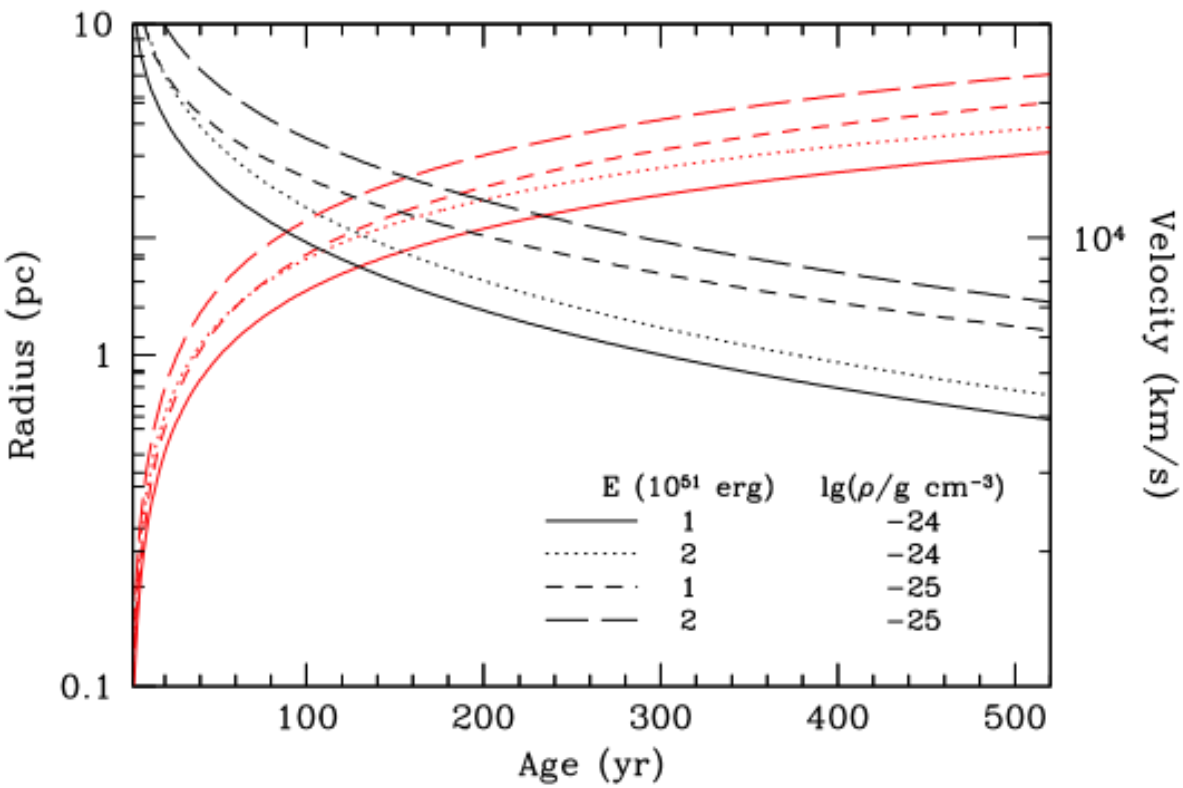

$$R_{ch} = \left(\frac{M_{ejecta}}{4/3\pi\rho_0}\right)^{1/3}$$

$$V_{ch} = \left(\frac{2\,E_{51}}{M_{ejecta}}\right)^{1/2}$$

$$t_{ch} = \frac{R_{ch}}{V_{ch}} = {M_{ejecta}}^{5/6}\,(4/3\pi\rho_0)^{-1/3}\,(2\,E_{51})^{-1/2}$$

Los Alamos NATIONAL LABORATORY EST. 1943
Managed by Triad National Security, LLC for the U.S. Department of Energy's NNSA
National Nuclear Security Administration
Unclassified

Hydrodynamic Model Comparison

1D Hydrodynamic Simulations: Similarity Solution

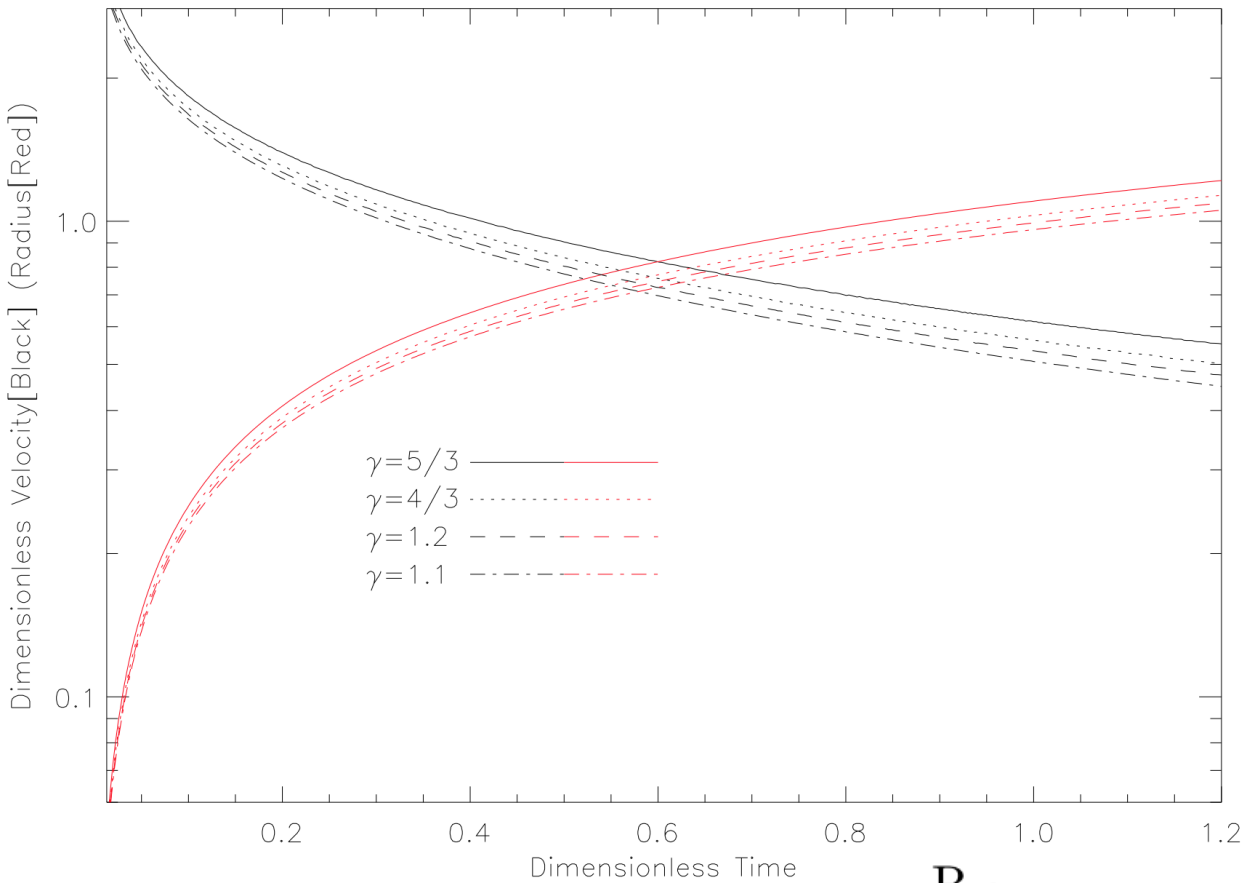

$$R_{ch} = \left(\frac{M_{ejecta}}{4/3\pi\rho_0}\right)^{1/3}$$

$$V_{ch} = \left(\frac{2\,E_{51}}{M_{ejecta}}\right)^{1/2}$$

$$t_{ch} = \frac{R_{ch}}{V_{ch}} = {M_{ejecta}}^{5/6}\,(4/3\pi\rho_0)^{-1/3}\,(2\,E_{51})^{-1/2}$$

Los Alamos NATIONAL LABORATORY EST. 1943
Managed by Triad National Security, LLC for the U.S. Department of Energy's NNSA
National Nuclear Security Administration
Unclassified

Hydrodynamic Model Comparison

Evolutionary Constraints from Models

Results

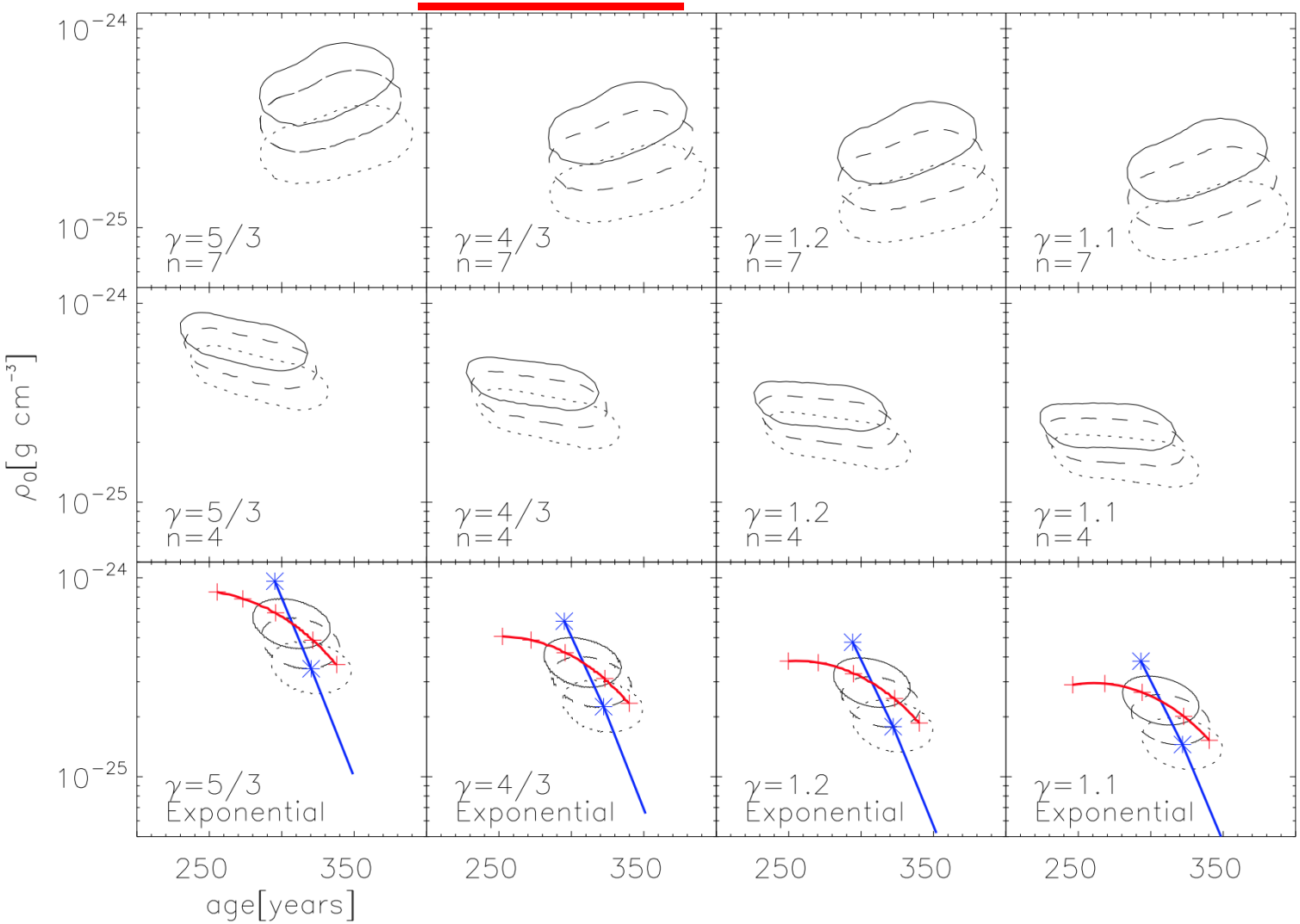

Hovey, Hughes, and Eriksen 2015

Hydrodynamic Model Comparison

Evolutionary Constraints from Models

Results

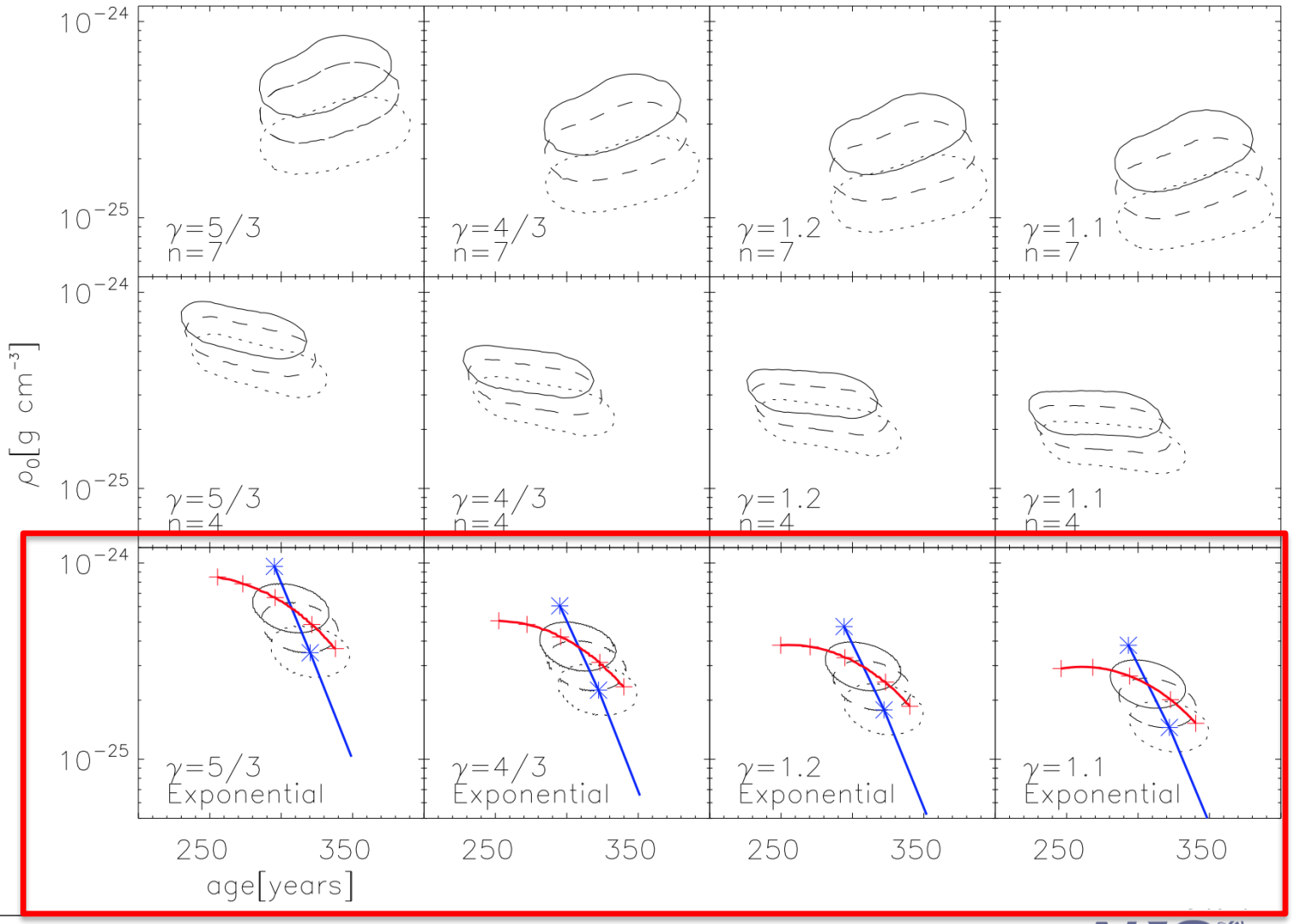

Hovey, Hughes, and Eriksen 2015

Hydrodynamic Model Comparison

Constraining the Shock Compression Ratio

Hovey, Hughes, and Eriksen 2015

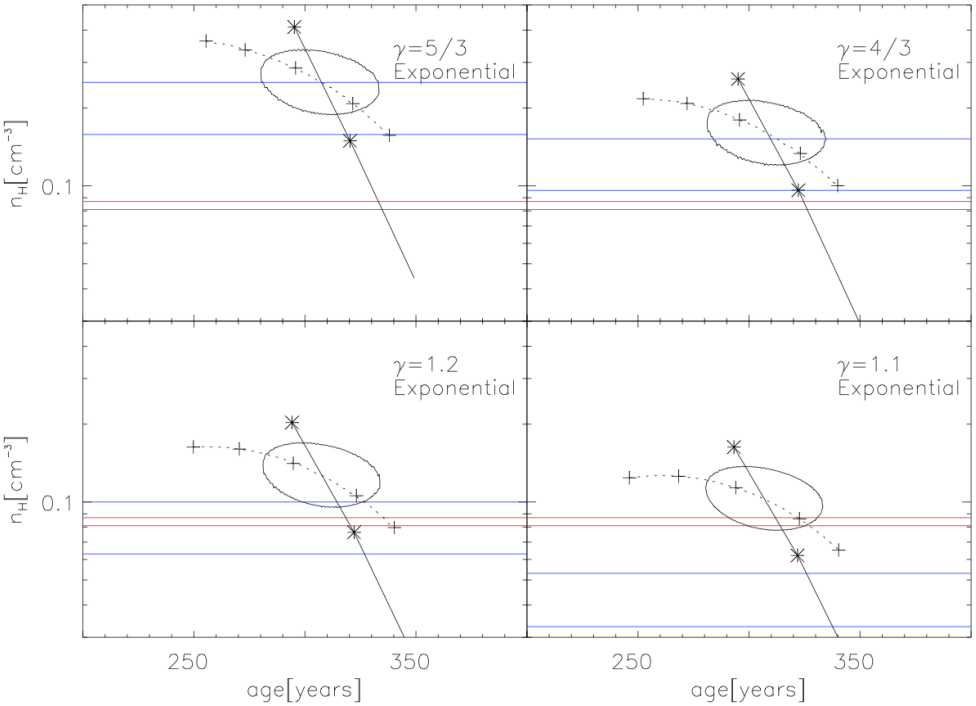

$\gamma_{\rm eff}$	C_γ	$\langle C_\gamma \rangle$	$n_{\rm H}$	$f_{\rm n}$
5/3	4	2.90±0.03	$0.203^{+0.048}_{-0.045}$	$0.41^{+0.098}_{-0.091}$
4/3	7	4.80±0.05	$0.123^{+0.029}_{-0.027}$	$0.68^{+0.102}_{-0.100}$
1.2	11	7.30±0.08	$0.081^{+0.019}_{-0.018}$	$1.04^{+0.250}_{-0.232}$
1.1	21	13.60±0.41	$0.043^{+0.010}_{-0.010}$	$1.95^{+0.478}_{-0.446}$

NOTE. — C_γ is the compression factor (ratio of post- to pre-shock density) at the forward shock. $\langle C_\gamma \rangle$ is the emission-measure-weighted compression factor, integrated from the contact discontinuity to the forward shock.

Hovey, Hughes, and Eriksen 2015

Hydrodynamic Model Comparison

Constraining the Shock Compression Ratio

Densities from IR dust measurements (Williams et al. 2011)

Hovey, Hughes, and Eriksen 2015

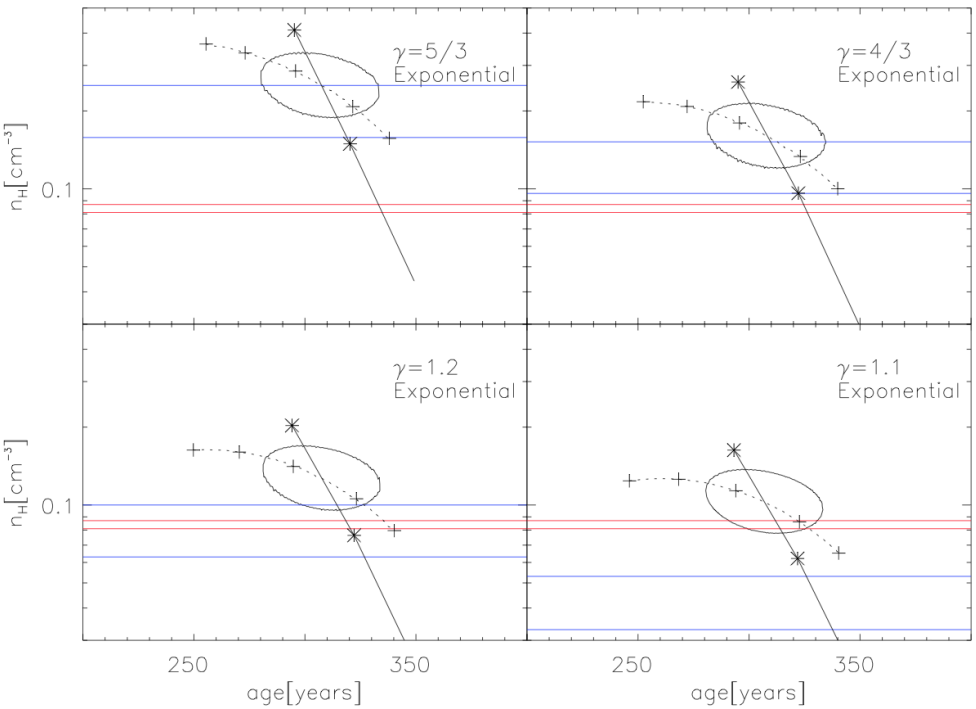

$\gamma_{\rm eff}$	C_γ	$\langle C_\gamma \rangle$	$n_{\rm H}$	$f_{\rm n}$
5/3	4	2.90±0.03	$0.203^{+0.048}_{-0.045}$	$0.41^{+0.098}_{-0.091}$
4/3	7	4.80±0.05	$0.123^{+0.029}_{-0.027}$	$0.68^{+0.102}_{-0.100}$
1.2	11	7.30±0.08	$0.081^{+0.019}_{-0.018}$	$1.04^{+0.250}_{-0.232}$
1.1	21	13.60±0.41	$0.043^{+0.010}_{-0.010}$	$1.95^{+0.478}_{-0.446}$

NOTE. — C_γ is the compression factor (ratio of post- to pre-shock density) at the forward shock. $\langle C_\gamma \rangle$ is the emission-measure-weighted compression factor, integrated from the contact discontinuity to the forward shock.

Hovey, Hughes, and Eriksen 2015

Hydrodynamic Model Comparison

Constraining the Shock Compression Ratio

From our neutral hydrogen density and n_H From Previous Column Densities from IR dust measurements (Williams et al. 2011)

$\gamma_{\rm eff}$	C_γ	$\langle C_\gamma \rangle$	$n_{\rm H}$	$f_{\rm n}$
5/3	4	2.90±0.03	$0.203^{+0.048}_{-0.045}$	$0.41^{+0.098}_{-0.091}$
4/3	7	4.80±0.05	$0.123^{+0.029}_{-0.027}$	$0.68^{+0.102}_{-0.100}$
1.2	11	7.30±0.08	$0.081^{+0.019}_{-0.018}$	$1.04^{+0.250}_{-0.232}$
1.1	21	13.60±0.41	$0.043^{+0.010}_{-0.010}$	$1.95^{+0.478}_{-0.446}$

NOTE. — C_γ is the compression factor (ratio of post- to pre-shock density) at the forward shock. $\langle C_\gamma \rangle$ is the emission-measure-weighted compression factor, integrated from the contact discontinuity to the forward shock.

Hovey, Hughes, and Eriksen 2015

Hovey, Hughes, and Eriksen 2015

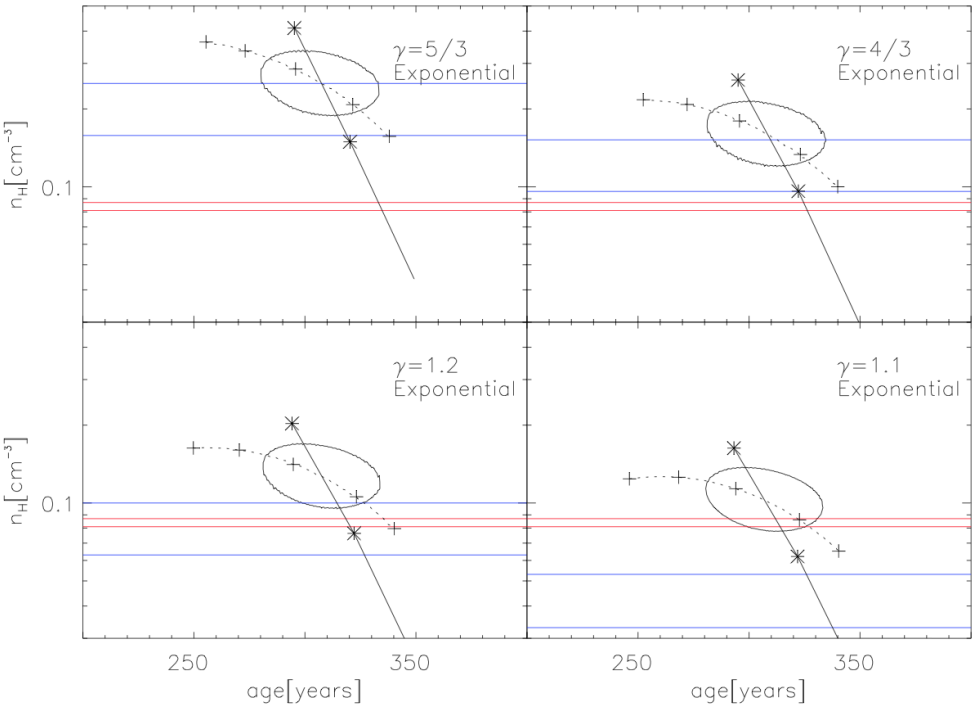

Hydrodynamic Model Comparison

Constraining the Shock Compression Ratio

From our neutral hydrogen density and n_H From Previous Column Densities from IR dust measurements (Williams et al. 2011)

Hovey, Hughes, and Eriksen 2015

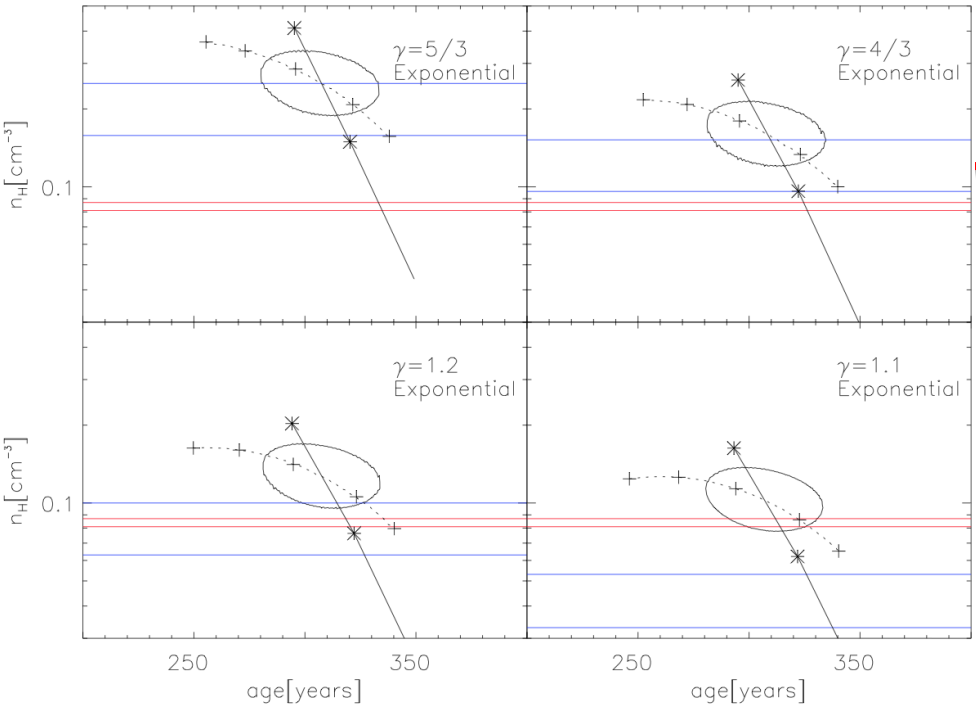

$\gamma_{\rm eff}$	C_γ	$\langle C_\gamma \rangle$	$n_{\rm H}$	$f_{\rm n}$
5/3	4	2.90±0.03	$0.203^{+0.048}_{-0.045}$	$0.41^{+0.098}_{-0.091}$
4/3	7	4.80±0.05	$0.123^{+0.029}_{-0.027}$	$0.68^{+0.102}_{-0.100}$
1.2	11	7.30±0.08	$0.081^{+0.019}_{-0.018}$	$1.04^{+0.250}_{-0.232}$
~~1.1~~	~~21~~	~~13.60±0.41~~	~~$0.043^{+0.010}_{-0.010}$~~	~~$1.95^{+0.478}_{-0.446}$~~

NOTE. — C_γ is the compression factor (ratio of post- to pre-shock density) at the forward shock. $\langle C_\gamma \rangle$ is the emission-measure-weighted compression factor, integrated from the contact discontinuity to the forward shock.

Hovey, Hughes, and Eriksen 2015

Hydrodynamic Model Comparison

Constraining the Shock Compression Ratio

From our neutral hydrogen density and n_H From Previous Column Densities from IR dust measurements (Williams et al. 2011)

Hovey, Hughes, and Eriksen 2015

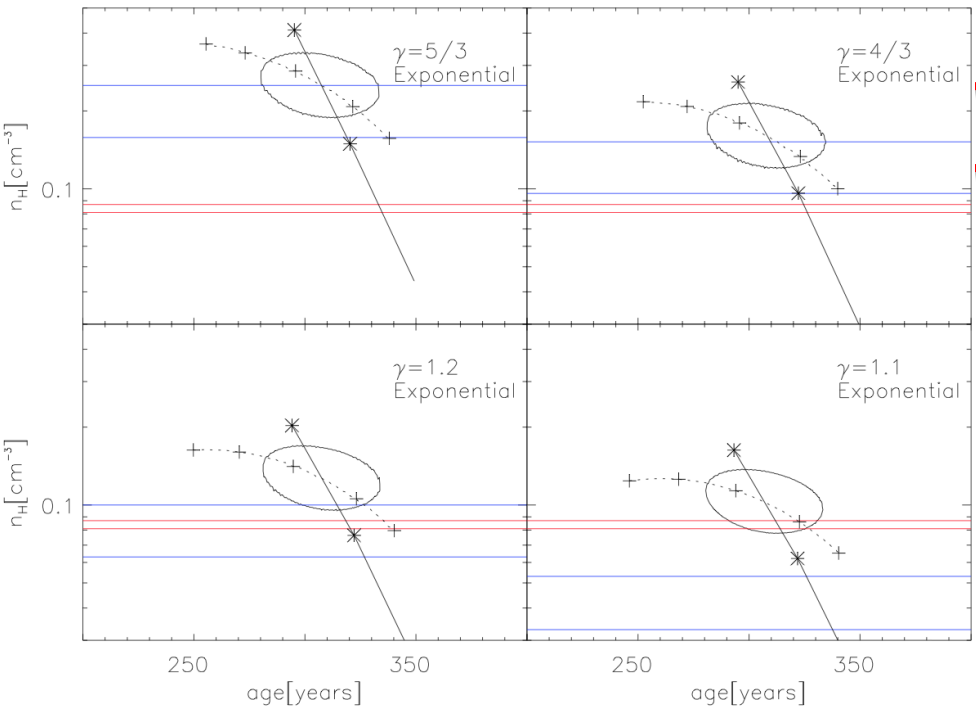

$\gamma_{\rm eff}$	C_γ	$\langle C_\gamma \rangle$	$n_{\rm H}$	$f_{\rm n}$
5/3	4	2.90±0.03	$0.203^{+0.048}_{-0.045}$	$0.41^{+0.098}_{-0.091}$
4/3	7	4.80±0.05	$0.123^{+0.029}_{-0.027}$	$0.68^{+0.102}_{-0.100}$
~~1.2~~	~~11~~	~~7.30±0.08~~	~~$0.081^{+0.019}_{-0.018}$~~	~~$1.04^{+0.250}_{-0.232}$~~
~~1.1~~	~~21~~	~~13.60±0.41~~	~~$0.043^{+0.010}_{-0.010}$~~	~~$1.95^{+0.478}_{-0.446}$~~

NOTE. — C_γ is the compression factor (ratio of post- to pre-shock density) at the forward shock. $\langle C_\gamma \rangle$ is the emission-measure-weighted compression factor, integrated from the contact discontinuity to the forward shock.

Hovey, Hughes, and Eriksen 2015

Conclusions: Part 1

- The global shock speed for the remnant is measured to be $v_s = 6500 \pm 200\ km\ s^{-1}$ for an assumed distance to the Large Magellanic Cloud being 50 kpc.
- Using this global shock speed we calculate a neutral hydrogen density of $\rho_{H_0} = 1.95 \pm 0.07 \frac{\epsilon_{h\alpha}}{0.2} \times 10^{-25} g\ cm^{-3}$
- Using our measured global shock speed and remnant size and comparing them to 1D hydro simulations we find an age of $310^{+40}_{-30}\ years$ for our preferred evolutionary model (initial exponential density distribution with an initial explosion energy of $E_0 = 1 \times 10^{51}$ ergs).
- We are able to use our measured shock speed, remnant speed, and our neutral hydrogen density results coupled with the post-shock hydrogen densities from Williams et al. 2011, to determine a maximum shock compression of $\frac{\rho_s}{\rho_0} \leq 7$.

Overview/Motivation

- A proper motion measurement of the young supernova remnant 0509-67.5 in the Large Magellanic Cloud
  - Image Processing
  - Linking Measured Observational Results to calculations and hydrodynamic Simulations
- Measuring the Spot Blur on Axis-2 at the Dual-Axis Radiographic Hydrodynamic Test Facility (DARHT)
  - Use of the Bayesian Inference Engine (BIE)
  - Real-world analysis of DARHT data

Bonus Slide

Balmer emission for Balmer-dominated Remnants

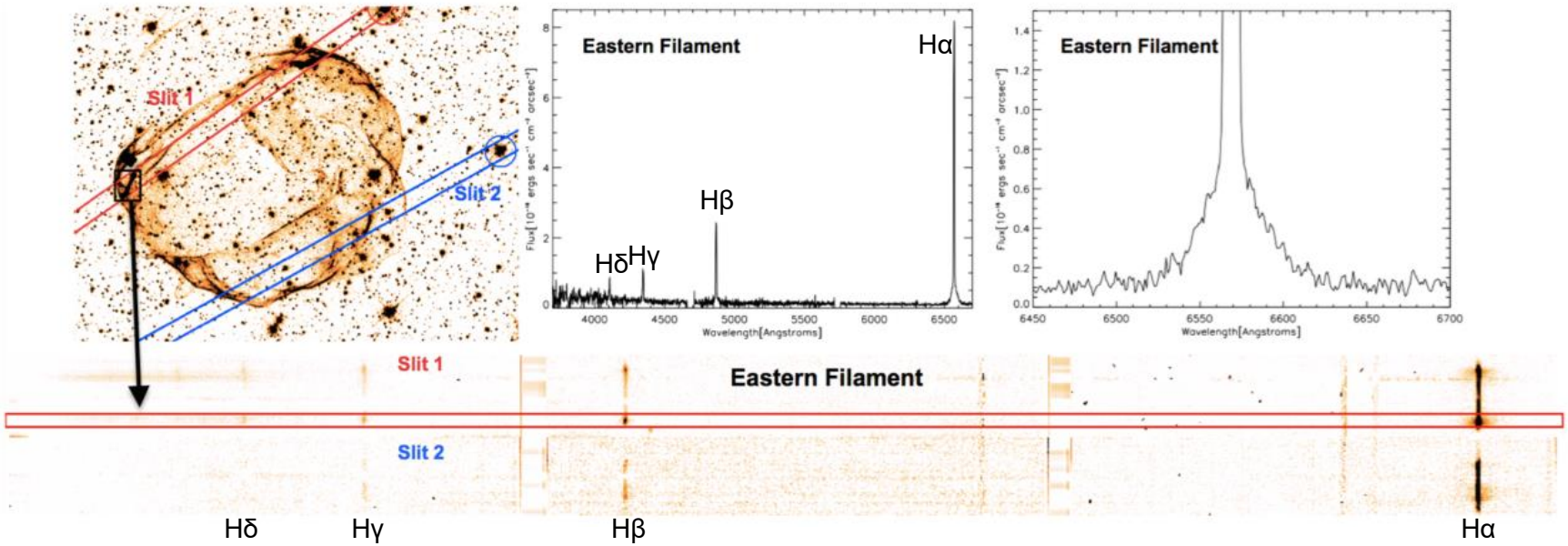

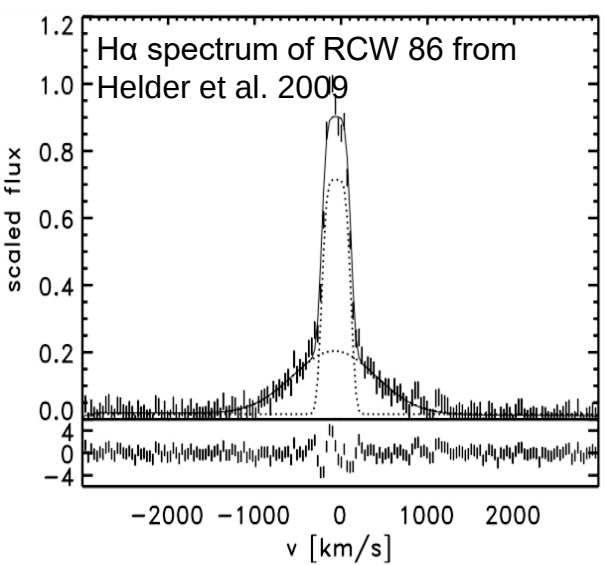

Bonus Slide

Balmer emission for Balmer-dominated Remnants

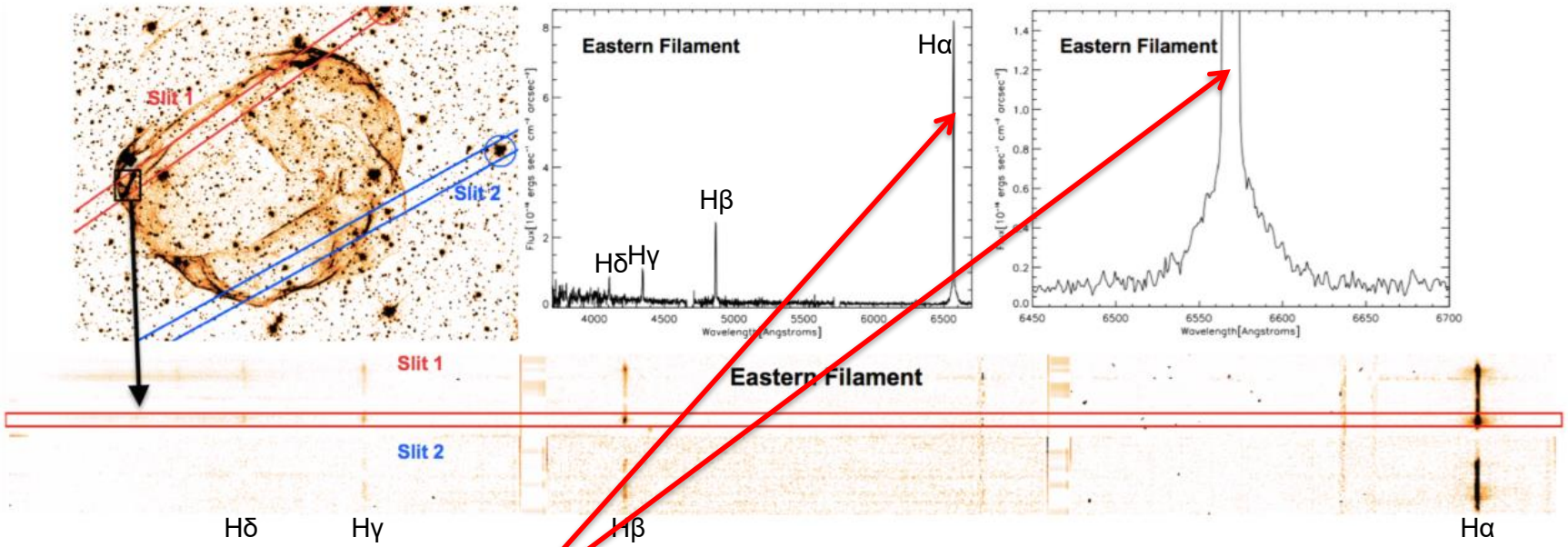

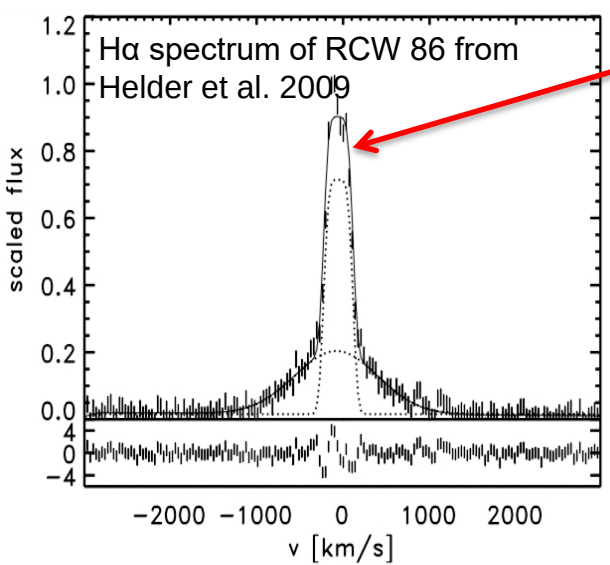

Narrow Hα – collisional excitations of hydrogen entering the forward shock

nt of Energy's NNSA
National Nuclear Security Administration
Unclassified

Bonus Slide

Balmer emission for Balmer-dominated Remnants

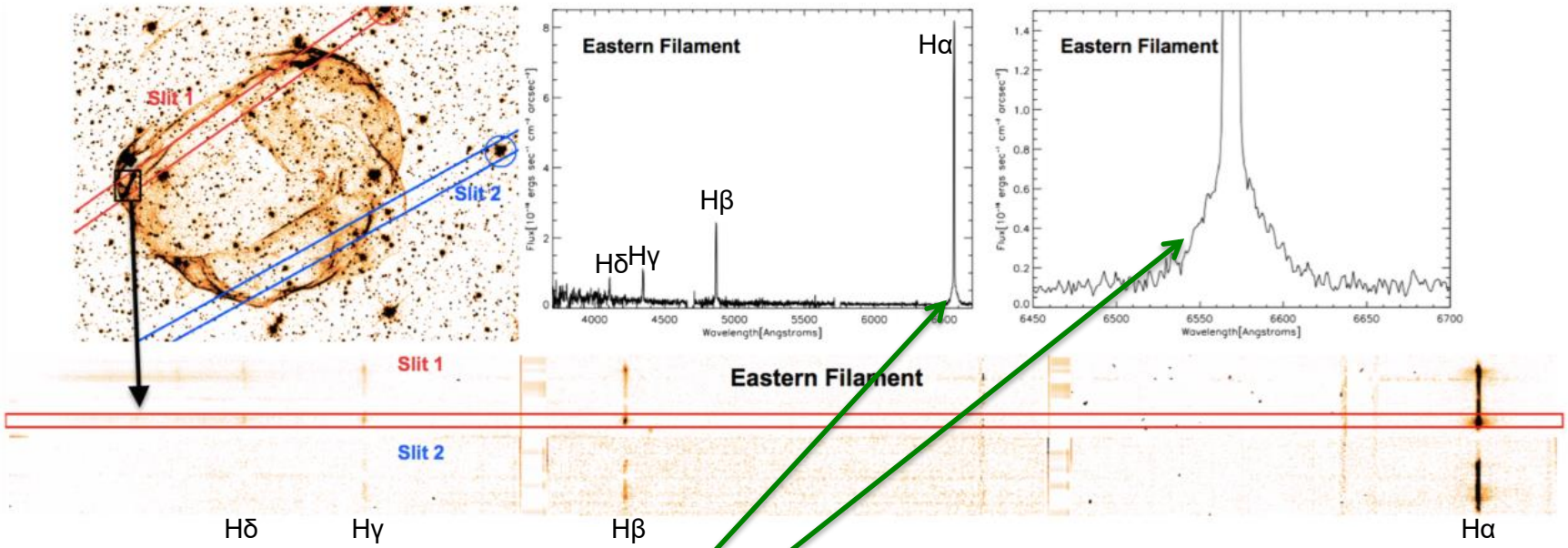

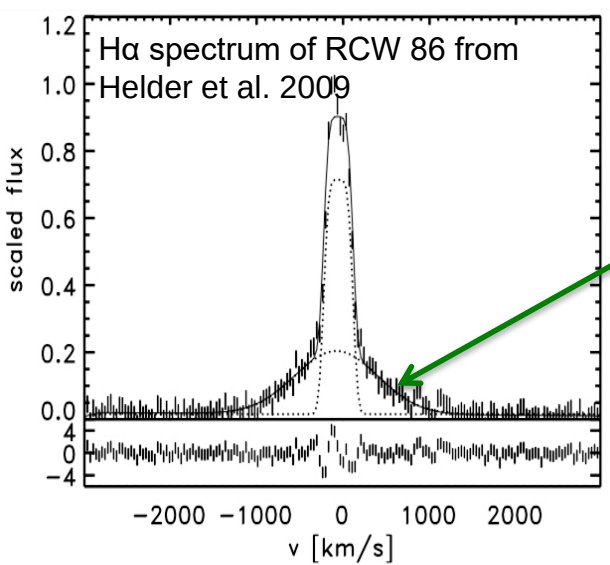

- Narrow Hα – collisional excitations of hydrogen entering the forward shock
- Broad Hα – Charge transfer from neutral hydrogen entering the forward shock that exchange their electron with a post-shock proton

nt of Energy's NNSA
Unclassified
National Nuclear Security Administration